The Canadian Mineralogist
Vol. 36, pp. 1485-1506 (1998)

SIGNIFICANCE OF *n*-ALKYLAMMONIUM EXCHANGE IN THE STUDY OF 2:1 CLAY MINERAL DIAGENESIS, MACKENZIE DELTA – BEAUFORT SEA REGION, ARCTIC CANADA

S. KELLY SEARS[1] AND REINHARD HESSE

Department of Earth and Planetary Sciences, McGill University, 3450 University Street, Montreal, Quebec H3A 2A7

HOJATOLLAH VALI

Electron Microscopy Centre, McGill University, 3640 University Street, Montreal, Quebec H3A 2B2

ABSTRACT

We have undertaken an XRD and HRTEM study of 2:1 clay minerals from argillaceous rocks of the Reindeer D–27 well, Mackenzie Delta – Beaufort Sea (MDBS) region, Arctic Canada. Separates of the fine clay fraction (<0.05 μm) after treatment with *n*-alkylammonium cations consist of 2:1 clay mineral assemblages which span the major steps in the evolution of smectite to illite (S → I). Diffraction patterns of the <0.05 μm fractions treated with octylammonium ($n_C = 8$) and octadecylammonium ($n_C = 18$) cations from intermediate (2659.4 m) to maximum depths (3832.8 m) in well D–27 suggest the presence of R1 and R3 ordered illitic phases. Lattice-fringe images reveal the presence of multiple metastable phases of low- and high-charge expandable 2:1 clay minerals, a short-range rectorite-like R1 ordered phase, "*n*-alkylammonium illite" and illite in zones that overlap with burial depth. Expandable 2:1 clay minerals decrease in abundance with depth of burial and were not observed in samples at maximum depth. Illitic and micaceous phases of variable layer thickness and origin are present at all depths. A rectorite-like R1 ordered phase dominates at the intermediate stage in the evolution of S → I at a depth of 2659.4 m, and apparently coherent sequences (packets) of illite with three to seven layers (R3 ordered) dominate at the maximum depth of 3832.8 m. Packets of "*n*-alkylammonium illite" are only identified in lattice-fringe images of samples from maximum well-depth. The prograde evolution of metastable 2:1 clay minerals with depth, which constitutes the conversion of *S* to I in the MDBS region, corroborates previous postulates that the principal mechanism of reaction is dissolution–crystallization.

Keywords: *n*-alkylammonium-cation exchange, smectite, rectorite-like R1 ordered phase, "*n*-alkylammonium illite", illite, HRTEM, XRD, Reindeer D–27 well, Mackenzie Delta – Beaufort Sea region, Arctic Canada.

SOMMAIRE

Nous avons entrepris une étude par diffraction X et par microscopie électronique en haute résolution d'argiles de type 2:1 provenant de roches argileuses traversées par le puit de forage Reindeer D–27, dans la région du delta de Mackenzie – mer de Beaufort, dans l'Arctique canadien. Les concentrés d'argiles de la granulométrie la plus fine (<0.05 μm), après traitement avec des cations *n*-alkylammoniac, contiennent des assemblages d'argiles à caractère 2:1 qui documentent les étapes majeures de l'évolution de smectite à illite (S → I). D'après les spectres de diffraction des fractions <0.05 μm traitées avec les cations octylammoniac ($n_C = 8$) et octadécylammoniac ($n_C = 18$) et provenant de profondeurs intermédiaires (2659.4 m) à maximales (3832.8 m) le long du puit D–27, les phases illitiques ordonnées R1 et R3 seraient présentes. Les images des franges réticulaires révèlent la présence de multiples phases métastables d'argiles gonflables 2:1 ayant une charge faible ou élevée, une phase à caractère ordonné à courte échelle rappelant la rectorite R1, illite de type "*n*- alkylammoniac" et illite, en zones qui se chevauchent en fonction de la profondeur d'enfouissement. Les argiles gonflables de type 2:1 diminuent en importance avec la profondeur, et semblent absentes dans les échantillons de profondeur maximale. Des phases illitiques et micacées à épaisseur de feuillet et origine variables sont présentes à chaque niveau le long du forage. Une phase ordonnée de type rectorite R1 est dominante à un stade intermédiaire de l'évolution de S à I à une profondeur de 2659.4 m, et des séquences apparemment cohérentes d'illite ayant de trois à sept couches (R3 ordonné) dominent à la profondeur maximale de 3832.8 m. Des empilements d'illite de type "*n*-alkylammoniac" ne sont identifiés que dans les images de franges réticulaires des échantillons prélevés des profondeurs maximales. L'évolution prograde des assemblages métastables d'argiles 2:1 avec la profondeur, qui mène à la conversion de

[1] *E-mail address*: sksears@canadamail.com

smectite en illite dans ce bassin sédimentaire, étaye l'hypothèse voulant que le mécanisme principal de la transformation implique une dissolution suivie d'une recristallisation.

(Traduit par la Rédaction)

Mots-clés: échange avec cations *n*-alkylammoniac, smectite, phase ordonnée de type rectorite R1, illite de type "*n*-alkylammoniac", illite, microscopie électronique en haute résolution, diffraction X, puit de forage Reindeer D–27, delta de Mackenzie, mer de Beaufort, Arctique canadien.

Introduction

The burial-diagenetic evolution of 2:1 clay minerals (low- and high-charge smectite, vermiculite, illite) in argillaceous rocks, and the nature and existence of interstratified illite–smectite (hereafter, IS), continue to generate scientific debate. There is interest in the potential role of IS as a geothermometer, and in the geological and economic consequences in clastic sedimentary basins of such interrelated phenomena as migration of hydrocarbons, generation of organic acids, development of secondary porosity, cementation by silica, evolution of geopressure, growth faulting and shale diapirism. Precise identification and characterization of the end-members and intermediate products in the diagenetic evolution of S → I in argillaceous rocks with increasing temperature and depth of burial are essential to determine the pathways and mechanisms of reaction, as well as the thermodynamic relationships, in order to model the kinetics of the reaction. Treatment of 2:1 clay minerals with *n*-alkylammonium cations has been shown to be superior to ethylene glycol and glycerol for the characterization in X-ray diffraction (XRD) and high-resolution transmission electron microscopy (HRTEM) of expandable 2:1 clay minerals (smectite and vermiculite) and the expandable component of IS of varying density of interlayer charge. The objectives of this study were to apply XRD and HRTEM to characterize and identify the 2:1 clay minerals after intercalation with *n*-alkylammonium cations separated from argillaceous rocks of the Beaufort – Mackenzie Basin (BMB) and the Brooks – Yukon Basin (BYB), frontier hydrocarbon basins located in Mackenzie Delta – Beaufort Sea (MDBS) region, Arctic Canada, and to document the mineralogical changes and relationships that constitute the S → I reaction with increasing temperature and depth of burial.

Background

Solid-state transformation and dissolution–crystallization are the two principal mechanisms that have been proposed to account for the structural and compositional changes that occur in 2:1 clay minerals during the diagenetic evolution of S → I in argillaceous rocks with increasing temperature and depth of burial. Perusal of the recent literature suggests that more than one mechanism of reaction may be operating, with multiple pathways and sequences of mineralogical and structural changes, which may be independent of one another, even when occurring in the same rock (*e.g.*, Pollastro 1985, Ahn & Peacor 1986a, Freed & Peacor 1992, Šucha *et al.* 1993, Ko & Hesse 1995, 1998, Lanson *et al.* 1998). The mechanism(s) of reaction in the evolution of S → I, however, is (or are) inexorably bound to the nature and relationship of the participating minerals (Altaner & Ylagen 1997, Moore & Reynolds 1997). Whereas most diagenetic studies of argillaceous rocks are in agreement that with increasing time, temperature, and depth of burial, illite is the eventual product if smectite is the original starting material, significant points of departure are the nature, relationship and characterization of the intermediate products and the mineralogical character of the illitic phases. Thus, the evolution of S → I has been viewed as a continuous or discontinuous series of actual illite and smectite layers interstratified within the IS crystallites (*e.g.*, Hower *et al.* 1976, Bell 1986), and as various physical mixtures or intergrowths of subpopulations of smectite, illite and short-range-ordered IS (Nadeau *et al.* 1985, Ahn & Peacor 1986a, Lanson & Champion 1991, Freed & Peacor 1992, Sears *et al.* 1995a, b, Dong *et al.* 1997). Closely related to the nature and relationship of the 2:1 clay minerals that constitute the S → I reaction is the true structure of the 2:1 clay minerals. On the basis of the response of 2:1 clay minerals to treatment with *n*-alkylammonium cations, Vali *et al.* (1994) concluded that the appearance of IS mixed-layers results from the arrangement and composition of polar and non-polar layers (Sudo *et al.* 1962, Tettenhorst & Johns 1965, Lippman & Johns 1969), and not from a mixture of illite and smectite layers. Lattice-fringe images of 2:1 clay minerals from diverse geological and pedological settings treated with *n*-alkylammonium cations showed smectite-group phases, vermiculite and "expandable illite" (hereafter "*n*-alkylammonium illite" or its variations; see below) as consisting of non-polar 2:1 layers. A rectorite-like R1 ordered phase is comprised of polar 2:1 layers only, and considered as a single phase (Lagaly 1979, Ahn & Peacor 1986b, Jiang *et al.* 1990, Jakobsen *et al.* 1995). Illite is comprised of both types of layers, having interior non-polar layers and exterior polar layers.

n-Alkylammonium Cation-Exchange Method

The stoichiometric exchange of interlayer cations in 2:1 layer silicates with *n*-alkylammonium cations enables the estimation of the density of interlayer cations,

layer charge and charge distribution of expandable 2:1 layer silicates, *e.g.*, smectite-group and vermiculite minerals (Lagaly & Weiss 1969, 1970, Lagaly 1981, 1982) and the expandable component of IS (Lagaly 1979, Müller-Vonmoos *et al.* 1994, Cetin & Huff 1995a). Treatment with *n*-alkylammonium cations also serves to stabilize the interlayers of expandable 2:1 clay minerals that otherwise collapse under the electron beam in the high vacuum of the TEM. Intercalation of other organic compounds, such as ethylene glycol and glycerol, in the interlayers of expandable 2:1 clay minerals are not stable in TEM (Ahn & Peacor 1986a, Bell 1986, Vali & Köster 1986).

The *n*-alkylammonium cation-exchange reaction and the degree of expansion are functions of alkyl chain-length ($6 \leq n_C \leq 18$, where n_C is the number of carbon atoms in an alkyl chain with the general formula $C_{n_C}H_{2n_C+1}NH_3^+$) and the density of interlayer charge. They also are influenced by the temperature of reaction, solution concentration, duration of incubation, chemical pretreatment, particle size and morphology, properties of the mineral, including the location of layer charge (tetrahedral *versus* octahedral), and conditions of washing (Lagaly 1981, 1994, Laird *et al.* 1987, Vali *et al.* 1991). In conventional models, at near room temperature, alkylammonium cations are oriented in the interlayer space of expandable 2:1 layer silicates (smectite and vermiculite) with the alkyl chains adopting an *all-trans* conformation, with a fixed cross-sectional area and the plane of the zigzag normal to (001), as flat-lying monolayers [$d(001)$ = 1.36 nm; Fig. 1a], bilayers [$d(001)$ = 1.77 nm; Fig. 1b], or pseudotrimolecular layers [$d(001)$ = 2.17 nm; Fig. 1c] (Lagaly & Weiss 1969, 1970, Lagaly 1981) [see Vaia *et al.* (1994) and Laird (1994) for alternative models]. Layer-charge heterogeneity, however, can lead to the appearance of non-integral interstratified spacings (*e.g.*, between 1.36 and 1.77 nm, or between 1.77 and 2.17 nm) in XRD patterns. In 2:1 layer silicates with a layer charge as low as >0.63 equivalents per half formula units, the alkyl chains have a paraffin-type orientation in the interlayer space [$d(001) > 1.9$ nm; Fig. 1d] (Lagaly 1982, Malla & Douglas 1987). The angle of tilt of the alkyl chains in a paraffin-type arrangement changes as a function of the number of carbon atoms in the chain and the density of the interlayer charge. Lagaly (1982) noted that the optimal orientation of the alkyl chains and molecular packing make the paraffin-type arrangement less sensitive to variations in charge density, making charge heterogeneity in higher-charge 2:1 layer silicates difficult to detect.

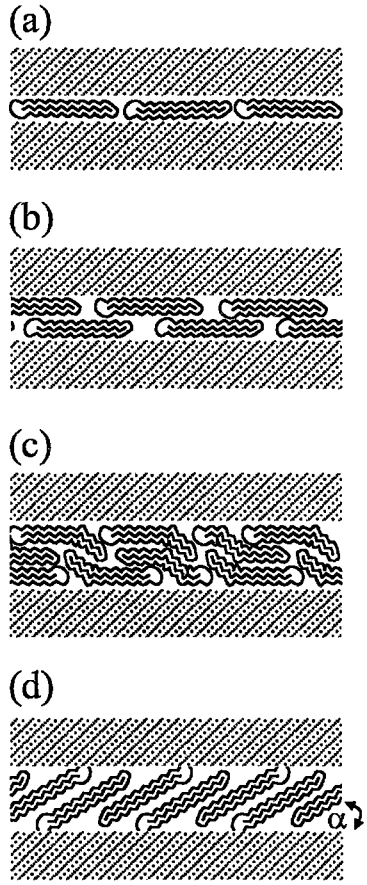

FIG. 1. Orientation and arrangement of alkyl chains (n_C = 16) in the interlayer space of 2:1 layer silicates: (a) monolayer, (b) bilayer, (c) pseudotrimolecular layer, (d) paraffin-type layer (α [angle of tilt] = 30°). After Lagaly & Weiss (1969) and Lagaly (1982). Not to scale.

"*n*-ALKYLAMMONIUM ILLITE"

Short- and intermediate-chain alkylammonium cations ($6 \leq n_C \leq 11$) are capable of rapidly intercalating in low- and high-charge 2:1 clay minerals, *e.g.*, smectite-group phases and vermiculite. Long-chain alkylammonium cations ($12 \leq n_C \leq 18$) are capable of selectively exchanging interlayer K and other cations, and thus, of expanding the interlayers of higher-charge 2:1 layer silicates such as mica, illite, glauconite, and the higher-charge component of IS, which are not expandable with ethylene glycol or glycerol (Weiss 1963, Mackintosh & Lewis 1968, Mackintosh *et al.* 1971, 1972, Lagaly 1979, Vali & Köster 1986, Laird *et al.* 1987, Vali *et al.* 1991, 1992, Müller-Vonmoos *et al.* 1994, Cetin & Huff 1995a, b) (Table 1). Long-chain alkylammonium mica and illite complexes, however, are probably non-stoichiometric and may have a limited range of composition (Weiss *et al.* 1993). Lagaly (1994) noted that intercalation of alkylammonium cations in the interlayer space of higher-charge 2:1 layer silicates may occur relatively rapidly, but is retarded or

TABLE 1. TYPICAL *d*(001) VALUES (nm) OF 2:1 LAYER SILICATES AFTER INTERCALATION OF VARIOUS ORGANIC MOLECULES, AS DETERMINED FROM XRD

2:1 Layer Silicate[1]	AD	EG	GLY	$n_C = 8$	$n_C = 18$
Smectite (low-charge)	1.5	1.7	1.8	1.36	1.77
Smectite (high-charge)	1.5	1.7	1.46	1.6[2]	2.17
Vermiculite (low-charge)	1.45	1.63	1.45	1.77	2.17
Vermiculite (high-charge)	1.42	1.43	1.42	1.9[3,4]	~2.9[4,5]
IS (R0 I[0.5]/EG-S)[6]	1.40	1.65	1.82	1.18	3.03
Illite	1.0	1.0	1.0	1.0	1.0/~2.9[4,7]
Mica[8]	1.0	1.0	1.0	1.0	1.0/~2.9[4,7]

[1] AD: air-dried; EG: ethylene glycol; GLY: glycerol (after Mg-saturation); $n_C = 8$: octylammonium cations; $n_C = 18$: octadecylammonium cations.
[2] Layer-charge heterogeneity can result in the appearance of non-integral interstratified *d*(001) values, *i.e.*, values between 1.36 and 1.77, or between 1.77 and 2.17.
[3] High-charge 2:1 layer silicates (>0.63 equivalents per half formula unit) may have a paraffin-type arrangement of alkylammonium cations.
[4] Angle of tilt (α) of the alkyl chains in the interlayer space is dependent on chain length and density of the interlayer charge.
[5] In HRTEM images, intercalated $n_C = 18$ vermiculite, illite or mica gives a *d*(001) value of ~2.4-2.5 nm.
[6] AD = $001_{1.4}/001_{1.0}$, EG = $001_{1.68}/001_{1.0}$, or GLY = $001_{1.78}/001_{1.0}$, $n_C = 8$ = $001_{1.36}/001_{1.0}$, $n_C = 18 = 001_{2.9}$.
[7] Treatment of illite and mica with long-chain alkylammonium cations generally produces two characteristic reflections representative of contracted and intercalated "alkylammonium illite" components (Vali *et al.* 1991).
[8] Muscovite generally shows limited intercalation of long-chain alkylammonium cations.

stopped after attaining a certain degree of exchange. Stanjek *et al.* (1992) reported that incomplete expansion of the interlayer in 2:1 clay minerals from soils after treatment with *n*-alkylammonium cations increased with decreasing particle-size, perhaps due to the polarizing effect of intercalated alkylammonium interlayers, *i.e.*, K is bound more tightly in interlayers adjacent to alkylammonium-expanded interlayers. The rate of K exchange may be more rapid in very thin packets of illitic phases than in thicker packets, as the geometrical constraints during the exchange process are not as strong in very thin packets (Lagaly, pers. commun. 1998, *cf.* Ross & Rich 1973, von Reichenbach 1973).

Long-chain alkylammonium-cation exchange of higher-charge 2:1 clay minerals is not a strictly kinetic phenomenon (duration and experimental procedure). Chemical analysis of illitic material from various geological and pedological environments revealed that apparently coherent sequences (packets) of illite that did not intercalate $n_C = 18$ into their interlayers had higher K and Al contents than packets of illite with intercalated $n_C = 18$ interlayers, which had lower, more variable K and Al contents (their Fig. 4). This finding suggests that illite has a range of composition.

The diagenetic evolution of S → I in argillaceous rocks of the Reindeer D–27 well, MDBS region, Arctic Canada, was investigated by comparing XRD patterns and lattice-fringe images of 2:1 clay minerals in the <0.05 μm fraction after treatment with short- and long-chain alkylammonium cations, octylammonium ($n_C = 8$) and octadecylammonium ($n_C = 18$), respectively. Application of these two chains is used to identify the various 2:1 clay mineral components by characterizing the structure and layer-stacking sequences of the *n*-alkylammonium 2:1 clay mineral complexes on the basis of their *d*(001) values, and the relative contribution of the various subpopulations of 2:1 clay minerals that constitute IS during the evolution of S → I in burial diagenetic sequences.

Location and Geological Setting

The Mackenzie Delta – Beaufort Sea (MDBS) region in northwestern Arctic Canada extends from approximately 68°N to the edge of the Canada Basin slope (72°N) and from 128° to 141°W (Dixon *et al.* 1994) (Fig. 2). The British American Oil Company, Shell Canada Limited and Imperial Oil Enterprises Limited (B.A. – Shell – I.O.E.) Reindeer D–27 well is located on the southeast end of Richards Island, Northwest Territories. It penetrates a Holocene to Albian siliciclastic succession consisting of alternating sandstone- and shale-dominated units of the Beaufort – Mackenzie Basin (BMB) and Brooks – Yukon Basin (BYB), to a depth of 3861.2 m (Dixon 1990, Dixon *et al.* 1992a). The only hydrocarbon show was a flow of gassy mud from the interval 2084.2 to 2089.4 m (Chamney 1971).

The siliciclastic sediments of the MDBS region resulted from the opening of the Canada Basin and the northward migration of sediment depocenters from cratonic foredeeps and deep-water troughs in front of the rising Cordilleran fold belt in the Late Aptian – Early Albian to the thermally subsiding, passive continental margin of the Beaufort Sea in the Late Maastrichtian and throughout the Cenozoic (Dixon *et al.* 1992a, b, Dietrich & Dixon 1997, McNeil 1997). Identification of basin-wide transgressive–regressive cycles allowed the Upper Cretaceous to Pleistocene siliciclastic succession of the BMB to be subdivided into eleven regionally extensive sequences (Dietrich *et al.* 1985, 1989, Dixon *et al.* 1985) (Fig. 3). Not all sequences, however, are present in the subsurface of the main delta area and the Reindeer D–27 well. These sequences include the Oligocene Kugmallit Sequence (134.1–317.0 m), the Late Eocene Richards Sequence (317.0–530.4 m), the Early to Middle Eocene Taglu (530.4–2712.7 m) and the Late Paleocene to Early Eocene Aklak (2712.7–3270.5 m) sequences (Reindeer supersequence), and the informally named Early to Middle Albian flysch formation (3270.5–3861.2 m) (Jeletzky 1971, Young *et al.* 1976, Dixon 1990, Dixon *et al.* 1992b, Dietrich *et al.* 1989, McNeil 1997, pers. commun. 1998). The siliciclastic succession in the area of the Reindeer D–27 well and the main delta region is currently experiencing erosion and uplift (Issler & Katsube 1994). Increases in porosity of the shale at ~2000 m and again at ~3710 m are attributed to zones of strong overpressure (Issler

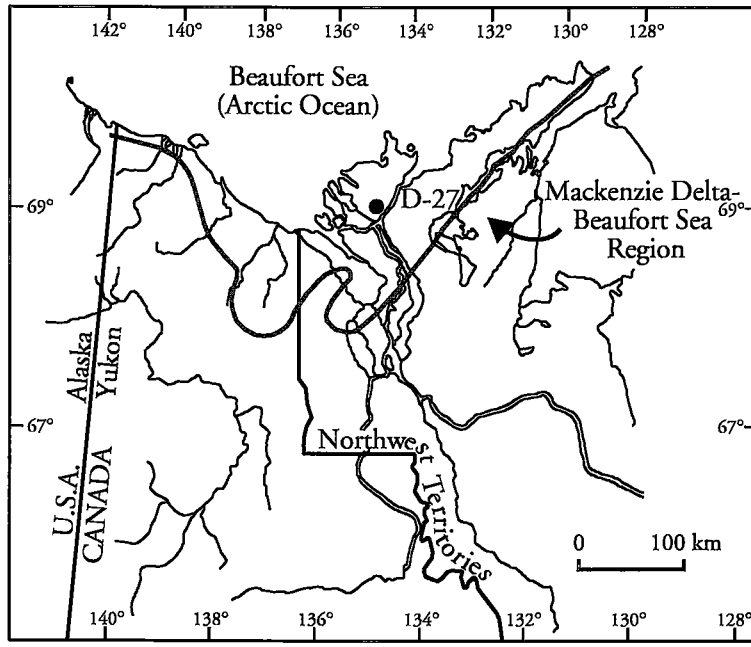

FIG. 2. Map showing the extent of the Mackenzie Delta – Beaufort Sea region and the location of the B.A. – Shell – I.O.E. Reindeer D–27 well on the southeast side of Richards Island, Mackenzie Delta, Northwest Territories, Arctic Canada.

1992) that may have been in existence since the Tertiary (Lane & Dietrich 1995). The present-day geothermal gradient of the Reindeer D–27 well was calculated at $27 \pm 5°C\ km^{-1}$ (J.A. Majorowicz, pers. commun, 1997). The paleogeothermal gradient in the MDBS region may have been similar to present-day values (Majorowicz & Dietrich 1989).

Materials and Analytical Techniques

Materials

Samples used for this investigation are drill core and hand-picked well cuttings of argillaceous rocks from the burial-diagenetic succession of the Reindeer D–27 discovery well, curated at the Geological Survey of Canada, Calgary, Alberta. Composite samples from cuttings were combined by weight extending over ~15 m (50 ft) intervals (Ko 1992). From eleven argillaceous rock samples that span almost the entire well-length, and include two core samples from 896.6 and 1463.0 m, one composite core-sample from 1920.2 to 1950.7 m, and eight samples of composite well-cuttings at intervals of ~300 m from 2057.4–2072.6 to 3825.2–3840.5 m, four samples were selected for detailed investigation: a core sample from 1463.0 m, a composite core sample from 1920.4 to 1950.7 m, and two samples of composite well-cuttings from 2636.5 to 2651.8 m and from 3825.2 to 3840.5 m. To simplify discussion, composite samples are identified by their median depth.

The samples were judged from diffraction studies to be representative, respectively, of the pre-diagenetic, early, intermediate and late stages of the S → I evolution. As diagenetic and detrital clay-mineral fractions in shales commonly are of similar size, and contamination by detrital material remains a persistent problem in the detection of diagenetic trends, the <0.05 μm size-fraction was chosen in an attempt to isolate 2:1 clay minerals and to minimize contamination from detrital illitic or micaceous phases.

Sample preparation

To avoid alteration of, and creation of artifacts in, the original clay material during sample preparation and separation, neither chemical treatment nor sonication was performed on the original argillaceous rock material. Core and well cuttings were washed in deionized water to remove drilling mud, and then disaggregated by mechanical agitation. The slurry was cleaned of excess electrolytes by repeated centrifugation until effective dispersion of particles was achieved. The <0.05 μm clay fractions were separated using a Sorvall SS–3 ta-

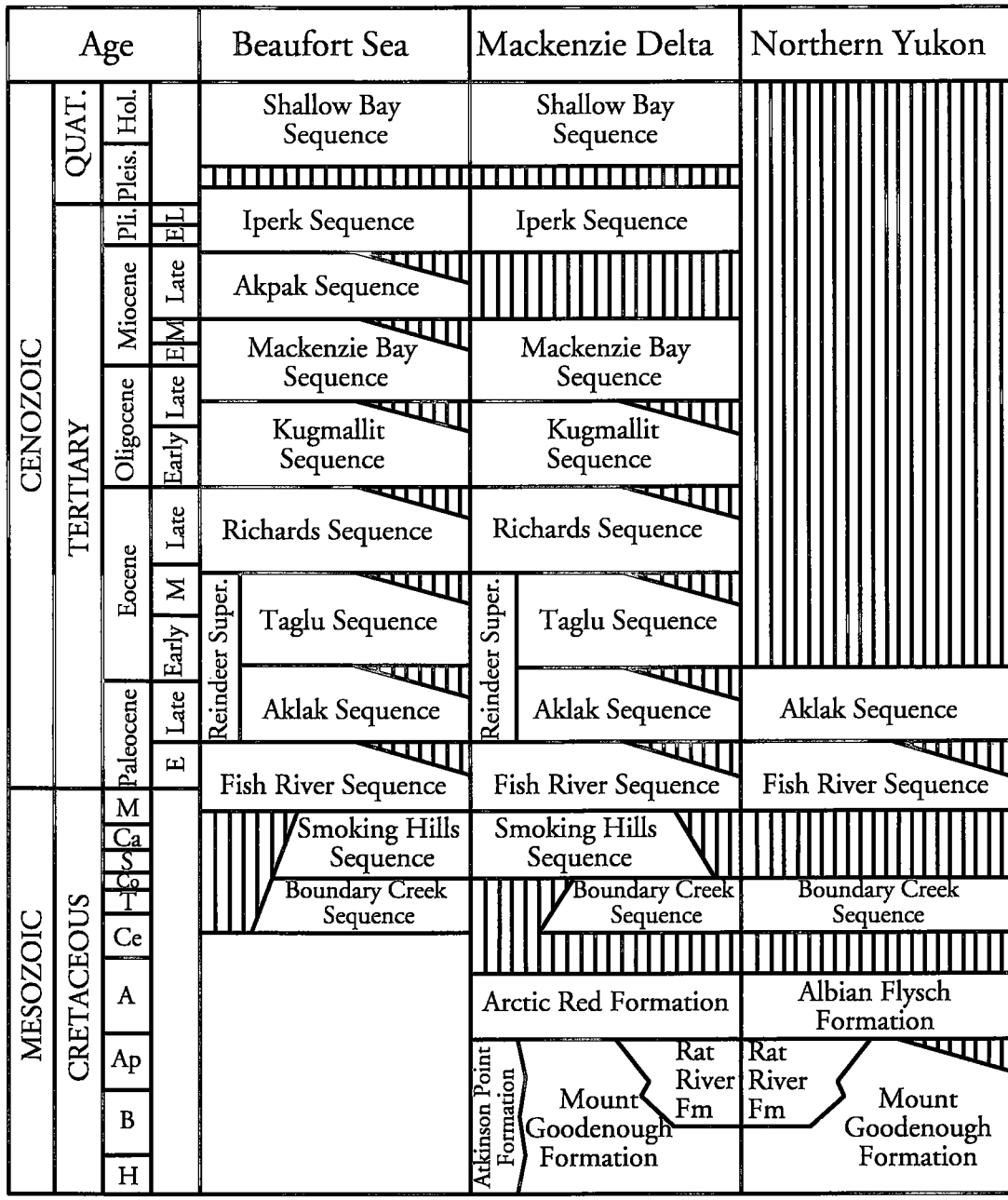

FIG. 3. Stratigraphic column of the Mackenzie Delta – Beaufort Sea (MDBS) region (after Dietrich & Dixon 1997). Not all sequences of the MDBS region are present in the subsurface of the main delta area and the Reindeer D–27 well.

ble-top centrifuge with a fixed-angle rotor and 250 mL centrifuge bottles. Dilute clay mineral suspensions were lyophilized in a Labconco 6 L freeze-dryer at –55°C and a vacuum of 10^{-3} torr.

Octylamine hydrochloride (n_C = 8) and octadecylamine hydrochloride (n_C = 18) were chosen both for their commercial availability, and for their ability to differentially expand low- and high-charge expandable 2:1 clay minerals and, in the case of n_C = 18, to selectively replace interlayer K in illitic and micaceous phases. Aqueous solutions with concentrations of 0.5 N for n_C = 8 and 0.05 N for n_C = 18 were prepared by dissolving the *n*-alkylamine hydrochloride in deionized water preheated to 65°C. Two procedures for alkylammonium cation-exchange were used on freeze-dried clay material: (i) before XRD analysis and HRTEM imaging, following the procedure of Rühlicke & Kohler (1981), or (ii) after embedding in a low-viscosity (60 centipoises) thermally curing epoxy resin (Spurr 1969) and preparation of ultrathin sections (Vali & Hesse 1990). Vali & Hesse (1992) reported no visible differences in the layer structure or organization of particles of phlogopite and vermiculite prepared by the two techniques. The high van-der-Waals interaction between the alkyl chains and the 2:1 layer silicates prevents the disintegration of the lattice during the exchange reaction (Lagaly 1981). Malla *et al.* (1993) noted, however, that the *n*-alkylammonium cation exchange of IS prior to embedding may result in the disruption of crystallites, *i.e.*, fewer layers (*c** direction) and smaller lateral extent (*a*–*b* plane) as compared with Na-saturated samples (*cf.* Laird & Nater 1993). The *n*-alkylammonium cation exchange of IS material after the preparation of ultrathin sections may prevent disintegration of the primary organization of layers and additional expansion from infiltration of organic molecules of resin into the alkylammonium-expanded interlayer space of 2:1 layer silicates.

Fifty milligrams of freeze-dried clay material were placed in glass centrifuge tubes and 10 mL of the appropriate solution of *n*-alkylamine hydrochloride added. Samples were incubated at 65°C for 24 hours, and repeatedly agitated during this period to resuspend the material, centrifuged at high speed (10,000 rpm); the supernatant was decanted, and the process was then repeated. After the second 48-hour incubation, *i.e.*, 5-day exchange period, the samples were washed with a 1:1 solution of 90% ethanol – H_2O and then washed 8 to 14 times in 90% ethanol to remove excess alkylammonium salts and alkylamines (Lagaly 1994).

Untreated samples were exchanged with Mg^{2+} by dispersing twice in a 1.0 M $MgCl_2$ solution and repeatedly washed with deionized H_2O followed by centrifugation. Oriented samples for XRD analysis were prepared from 15–20 mg of Mg-saturated clay separates dispersed in 5 mL of deionized H_2O using a modified version of the membrane-filter transfer method (Drever 1973, Pollastro 1982). The procedure was simplified by retaining the filter and mounting on a glass slide with diluted white glue (Sears 1993, *cf.* McAlister & Smith 1995). The samples were solvated with ethylene glycol (EG) by vapor pressure at 60°C for 24 hours and immediately X-rayed. The *n*-alkylammonium 2:1 clay minerals were dispersed in ~1 mL of a 1:1 90% ethanol – deionized H_2O solution, pipetted onto glass slides, and allowed to dry at room temperature. The slides were placed in the freeze-dryer under high vacuum overnight and immediately X-rayed.

After XRD, the 2:1 clay mineral samples (either Mg-saturated or treated with *n*-alkylammonium cations) were embedded in Spurr resin following a procedure modified from Lee *et al.* (1975). Approximately 10–20 mg of clay separate was placed in 1.5 mL polypropylene Eppendorf micro test tubes and dehydrated by adding ~1 mL propylene oxide to remove adsorbed water. After high-speed centrifugation (10,000 rpm), the propylene oxide was decanted, and 100% Spurr resin was added. The micro test tubes were agitated for 24 hrs to ensure complete impregnation; the resin–clay mixture was transferred to embedding moulds and cured at 65° for 24 hours. Ultrathin sections were cut from the resin blocks using an LKB Ultratome III ultramicrotome equipped with a Diatome diamond knife. Selected sections were transferred to the center of 300 mesh Cu TEM grids with formvar and carbon-supported film (Vali & Köster 1986, *cf.* Marcks *et al.* 1989).

For 2:1 clay-mineral separates not previously treated with *n*-alkylammonium cations, grids containing ultrathin sections were transferred to 1.5 mL micro test tubes containing 1.0 mL of the *n*-alkylammonium-cation solution diluted to 40–50% of the initial concentration (see above) (Vali & Hesse 1990). The tubes were placed in an oven at 65°C for 20 minutes and agitated every few minutes to ensure complete exchange of cations. The grids were then washed 8–14 times with deionized H_2O preheated to 65°C. Precipitation of free alkylammonium salts and alkylamines on the ultrathin section and corrosion of the Cu grid may occur if the concentration of the *n*-alkylammonium solution is too high and the duration too long, or if the solution is allowed to cool during washing (the use of Ni or Au grids will alleviate some of these problems).

XRD and TEM analysis

XRD analysis was performed on a Siemens D–500 automated diffractometer equipped with a graphite diffracted-beam monochromator (Cu*K*α radiation) using the following analytical conditions: operating voltage of 40 kV, beam current of 20 mA, step-size of 0.01° 2θ, counting time of 1 second per step, 0.15 mm receiving slit, and a scanning range of 2 to 40° 2θ. The proportion of expandable interlayers and type of order of IS were estimated from the experimental XRD patterns of Mg-saturated and EG-solvated samples using the Δ2θ method of Moore & Reynolds (1997) and by compari-

son with calculated patterns generated with the program NEWMOD© (Reynolds 1985).

All ultramicrotomed samples were imaged in bright-field illumination at high resolution with a JEOL JEM–100 CX II transmission electron microscope (TEM) at an accelerating voltage of 100 kV. The phase contrast of one-dimensional lattice-fringe images of clay minerals with focus conditions approximating Scherzer defocus depends on the structure and thickness of the specimen and instrumental conditions. Magnification ranged between 20,000 and 100,000×. Although only a few images are presented, results are based on hundreds of images taken, and represent some commonly observed features.

HRTEM interpretation of layer sequences of 2:1 clay minerals after treatment with n-alkylammonium cations

HRTEM is very useful to document and image the evolution of 2:1 clay minerals in a burial-diagenetic succession with increasing temperature and depth. Differences in the layer arrangement of interstratified 2:1 clay minerals are apparent when alternative focus conditions are employed. Distinction between expanded and non-expanded interlayers in interstratified structures and detection of compositional periodicity (1–D ordering of cations) are possible if one uses overfocus (compositional focus) and image simulation (Guthrie & Veblen 1989, 1990, Veblen *et al.* 1990). Image simulation of ordered IS, assuming a smectitic structural formula, suggests that in compositional imaging, thin dark fringes correspond to illitic interlayers, and thick dark fringes correspond to collapsed expandable interlayers, *e.g.*, of smectitic character, but the fringes do not directly overlie 2:1 silicate layers (Guthrie & Veblen 1990). In contrast, Scherzer defocus (underfocus) of 2:1 clay minerals can be used to acquire structural information, *i.e.*, information on the arrangement of layers and interlayers. Dark fringes approximately overlie regions of relatively high density (2:1 silicate layers), and bright fringes approximately overlie regions of relatively low density (interlayers).

The effect of a change from Scherzer defocus to overfocus is illustrated by Figures 4a and 4b, which reveal striking differences in the structural arrangement of free particles present in the images. The images of dispersed 2:1 clay minerals after treatment with $n_C = 18$ were photographed within seconds of each other under identical TEM operating conditions. The lattice-fringe image at Scherzer defocus shows predominantly curved or wavy, single 2:1 silicate layers, characteristic of elementary particles of smectite, isolated double layers (two 2:1 silicate layers) with a non-expanded interlayer (interfaces are expandable with *n*-alkylammonium cations), considered to be a rectorite-like R1 ordered phase (Vali *et al.* 1994), and apparently coherent sequences (packets) of 2:1 silicate layers with two or more non-expanded interlayers, characteristic of illite (Fig. 4a). As Vali *et al.* (1994) proposed, the smallest unit of illite consists of three 2:1 silicate layers, whereas two 2:1 silicate layers constitute the smallest unit of a rectorite-like R1 ordered phase, and a single 2:1 silicate layer is a smectite. It is expected that smectite would be abundant at this shallow depth of burial, as predicted from the Mg-saturated, EG-solvated XRD pattern. In contrast, the overfocus image shows the predominance of particles with apparently two 2:1 silicate layers and thicker par-

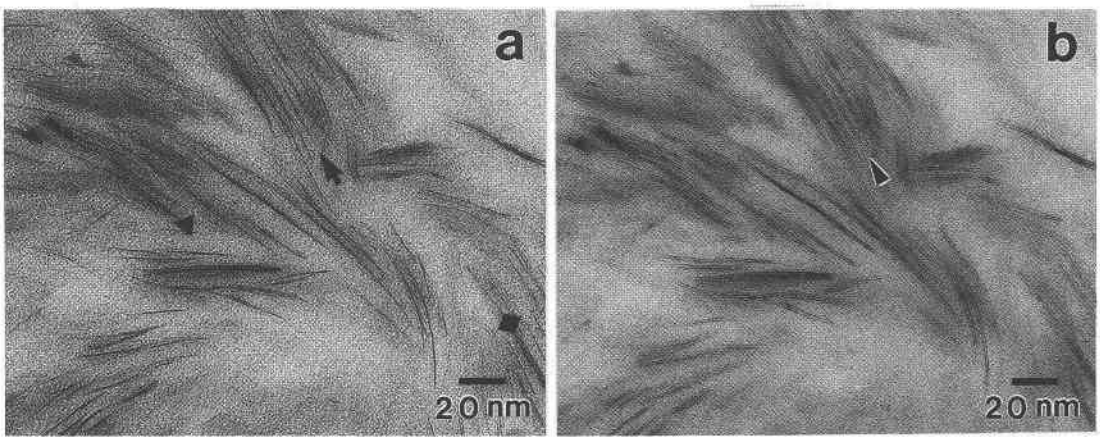

FIG. 4. HRTEM images of the <0.05 μm size fraction from 1463.0 m after treatment with $n_C = 18$: (a) at Scherzer defocus, the sample contains single layers of smectite (short black arrow), double layers of a rectorite-like R1 ordered phase (triangle) and apparently coherent sequences (packets) of illite (diamond); (b) at overfocus, the single layers of the smectite-group phase in (a) appear as two layers (black arrow with white border) (see text for further discussion).

ticles of apparently coherent packets of 2:1 silicate layers with non-expanded interlayers (Fig. 4b). Image simulation is required, however, to accurately interpret the structure. In samples treated with *n*-alkylammonium cations, the single 2:1 silicate layers observed at underfocus appear in overfocus as two 2:1 silicate layers with non-expanded interlayers. Single 2:1 silicate layers (smectite) are not observed in any sample at any depth in overfocus conditions. As single layers of smectite are expected to occur, especially at shallow depths, and since single 2:1 silicate layers after *n*-alkylammonium cation exchange are observed only at Scherzer defocus, we contend that this is the optimal condition to image and differentiate expanded and non-expanded 2:1 layer silicates after *n*-alkylammonium cation exchange.

It follows from the above discussion that crystal orientation, thickness, and focus conditions are crucial to a reliable interpretation of the layer arrangement and structure, as well as lattice spacing of 2:1 clay minerals in HRTEM images after treatment with *n*-alkylammonium cation. For example, Laird & Nater (1993) suggested that they observed, in HRTEM images of soil samples, two-layer elementary illite particles after treatment with a 0.065 M solution of octadecylamine hydrochloride (n_C = 18) for three hours (their Figs. 4, 5). We contend, however, that these particles represent sequences of an expandable 2:1 clay mineral with intercalated n_C = 18 interlayers. It is more likely that the appearance of an additional "layer" within the expanded interlayers is an artifact of focusing and orientation of the 2:1 clay minerals, and results in misidentification of sequences of an n_C = 18 high-charge expandable 2:1 layer silicate with a thickness of 2.02 nm, as non-expanded two-layer particles of elementary illite.

There is some inconsistency in the *d*(001) spacings of "octadecylammonium illite" and mica determined from XRD patterns and HRTEM images (Vali *et al.* 1991). Illite and mica having interlayers intercalated with n_C = 18 in a paraffin-type arrangement generally have a *d*(001) of 2.9 to 3.1 nm (*e.g.*, ~1.0 nm 2:1 layer silicate + 1.9 nm intercalated n_C = 18 interlayer) in XRD, whereas in HRTEM images, *d*(001) is measured as ~2.4–2.5 nm (~1.0 nm silicate layer + ~1.4 nm intercalated n_C = 18 interlayer). This discrepancy may be the result of the evaporation of ammonia from the decomposition of alkylammonium cations by the electron beam in TEM.

Owing to the extensive variation in the density of interlayer charge of smectite and rectorite-like R1 ordered phase, however, the spacings of intercalated alkylammonium interlayers can show considerable variation (Vali *et al.* 1994), making distinction between "*n*-alkylammonium illite" difficult. In addition, infiltration of embedding resin into the interlayer space of expandable 2:1 clay minerals previously intercalated with alkylammonium cations may result in additional expansion (Laird *et al.* 1989). Textural criteria and order of stacking of particles are used as additional tools to distinguish smectite and illitic phases treated with *n*-alkylammonium cations. Thus in the lattice-fringe images of this study, low-charge smectite is identified as dispersed single layers, and high-charge expandable 2:1 clay minerals, as sequences of curved or wavy layers with intercalated interlayers of up to 3.0 nm, and "octadecylammonium illite" with intercalated n_C = 18 interlayers of ~2.4–2.5 nm. Using the modified "Reichweite" notation of Vali *et al.* (1994) in terms of the structural arrangement of polar and non-polar mixed-layers, R0 represents a random mixed-layer structure, R1 is a rectorite-like structure, R3 represents an ordered sequence with 3 to 7 layers of illite, and R > 1 is a structure intermediate between that of R1 and R3.

Results and Discussion

Clay mineralogy of the <0.05 μm size fraction determined from conventional XRD analysis (Mg-saturated, ethylene glycol-solvated)

The experimental XRD patterns of the Mg-saturated and EG-solvated <0.05 μm fractions display features similar to patterns of clay minerals from pedogenic environments. In particular, they show a reduced intensity, unusual broadness and overlapping peaks owing to very thin crystallites and the small amount of material available in the <0.05 μm size-fraction, with displacement of peak position and changes in shape resulting from increased intensity of the background. Although the comparison of experimental and calculated XRD patterns reveals a similarity in peak positions, intensity values are more than an order of magnitude greater in the calculated patterns (Sears 1993).

A conventional XRD analysis indicates that the dominant clay mineral is an IS with a progressive increase in illite layers with depth of burial. The composition ranges from random IS with 40% illite layers [R0 illite(0.40)/EG-smectite] at 1463.0 m to R1 illite(0.70)/EG-smectite at 2949.0 m. At 3253.8 m, there is an apparent decrease to R1 illite(0.60)/EG-smectite, whereas at 3848.1 m, an increase to R > 1 illite(0.80)/EG-smectite occurs (see Sears *et al.* 1998, Fig. 1). Diffraction patterns of the <0.1 μm fractions after K-saturation (Ko & Hesse 1995) and the <0.05 μm fraction after Mg-saturation and glycerol solvation (Sears 1993) indicated that a minor amount of a high-charge expandable 2:1 clay mineral (smectite or vermiculite) component is also present. These results are in accordance with Powell *et al.* (1978), who concluded that in the <0.2 μm size fraction from argillaceous rocks of the Reindeer D–27 well, IS consisted of a three-component system of interstratified smectite – vermiculite – illite. Those authors further suggested that smectite transformed to illite through an intermediate step involving vermiculite (*e.g.*, interstratified vermiculite–illite), although the abundance of the vermiculite component remains fairly con-

stant with depth. Minor kaolinite is present in shallow samples, whereas minor chlorite is present in samples below the mineralogical discontinuity, but whether this is diagenetic or inherited (detrital) in origin remains uncertain (Sears 1993).

XRD analysis and TEM imaging of 2:1 clay minerals after treatment with n-alkylammonium cations: 1463.0 m

XRD analysis of the Mg-saturated and EG-solvated <0.05 μm clay mineral separates from 1463.0 m suggests an R0 illite(0.40)/EG-smectite. As expected, the diffraction pattern of the sample after $n_C = 8$ exchange is similar to the diffraction pattern of the Mg-saturated, air-dried sample (Figs. 5a). Using NEWMOD©, the calculated powder-diffraction pattern suggests that the observed reflections at 1.37, 0.65, 0.46 and 0.335 nm in the experimental pattern represent the non-integral composite positions and intensities of an IS with intercalated $n_C = 8$ arranged in the interlayers as monolayers. Cetin & Huff (1995a) reported a close correlation between expandability estimated from experimental XRD patterns of illite/EG-smectite and calculated XRD patterns of illite/EG-smectite and of illite/short-chain alkylammonium smectite. Complete agreement between experimental and calculated two-component diffraction patterns of samples treated with $n_C = 8$ could not be achieved in this study because of the probable addition of a high-charge expandable 2:1 clay mineral. Short-chain alkylammonium cations orient themselves as bilayers and pseudotrimolecular layers in the interlayer

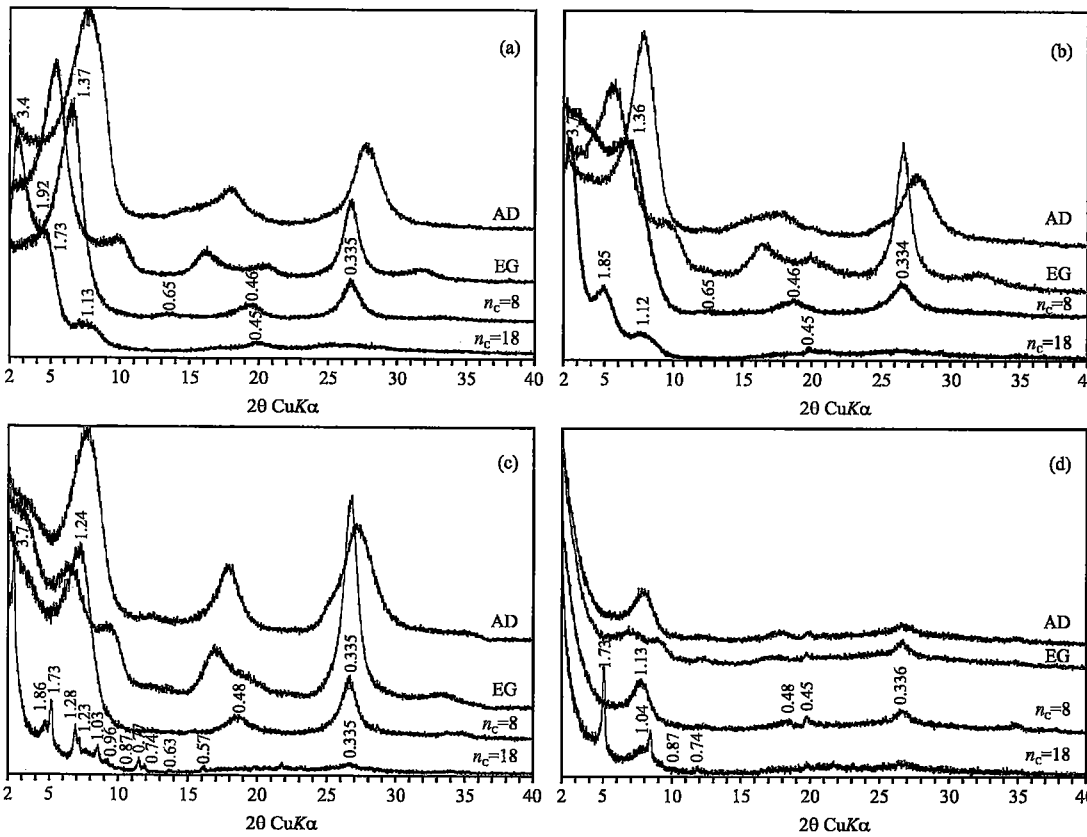

FIG. 5. XRD patterns of the <0.05 μm size-fraction separated from argillaceous of the Reindeer D–27 well from: (a) 1463.0 m (core), (b) 1935.4 m (core), (c) 2659.4 m (well cuttings), and (d) 3832.8 m (well cuttings). The diffraction patterns of samples treated with alkylammonium cations ($n_C = 8$ and $n_C = 18$) shown in (b) were performed on a Rigaku D/Max 2400 12 kW rotating anode X-ray diffractometer at 40 kV and 120 mA, with a receiving slit of 0.15 mm, step-size of 0.04° 2θ and a counting time of 0.6 second per step. The raw files (.MDI) were processed with JADE+ (Materials Data, Inc., Livermore, CA), exported as .PLT files, and printed using CorelDRAW! 7.0. (AD: air-dried, EG: ethylene glycol; $n_C = 8$, octylammonium cations; $n_C = 18$, octadecylammonium cations.)

space of high-charge smectite, and as a paraffin-type arrangement in vermiculite (Table 1). A comparison of the $n_C = 8$ pattern with that of the air-dried sample shows that reflections have shifted to lower 2θ angles, suggesting the incorporation of a high-charge expandable 2:1 clay mineral component. Thus, the broad reflection at 1.37 nm may be a mixture of three 2:1 clay minerals: a high-charge expandable 2:1 clay mineral with a basal spacing of a 1.77, a low-charge smectite with a $d(001)$ of 1.36 nm, and illite with a $d(001)$ of 1.0 nm ($001_{1.77}$/$001_{1.36}$/$001_{1.0}$ peak). These three components are observed in the lattice-fringe images after treatment with $n_C = 8$, as high-charged 2:1 layer silicates are not expanded by short-chain alkylammonium cations ($n_C < 12$) (see below).

The XRD pattern of the sample from 1463.0 m after treatment with $n_C = 18$ is dominated by a peak of ~3.4 nm with a higher-angle shoulder of 1.92 nm (Fig. 5a). Thus it appears that a phase that did not respond to $n_C = 8$ is responding to $n_C = 18$. A noticeable broad hump exists between 6° and 9° 2θ and is present in all samples of this study treated with $n_C = 18$. It may, however, also have superimposed sharp reflections (see below). The reflection of ~3.4 nm (001)* suggests a superlattice reflection with the integral higher-order reflections of ~1.73 (002)* and 1.13 (003)* nm, but owing to overlapping reflections in the low-angle range, the basal spacings cannot be easily deciphered. A reflection at ~3.4 nm suggests an R1-ordered structure, which consists of one 2:1 silicate layer (1.0 nm) and one 2:1 silicate layer with an $n_C = 18$-expanded interlayer of ~2.4 nm (1.0 + 2.4 = 3.4 nm). The intercalated $n_C = 18$ interlayer suggests an intermediate to high density of interlayer charge typical of vermiculite with a paraffin-type arrangement of the alkyl chains. Lagaly (1979) reported a $d(001)$ of >3.1 nm for a rectorite-like R1 IS after treatment with octadecylammonium cations (his Fig. 3). Velde (1985) suggested that the expandable layers in rectorite commonly consist of a high-charge smectite component. A $d(001)$ of 3.4 nm is too large to be an apparently coherent sequence of intercalated $n_C = 18$ interlayers, *e.g.*, octadecylammonium vermiculite would have a $d(001)$ of ~2.9 nm. It also cannot represent an R > 1 ordered structure, *e.g.*, two 2:1 silicate layers (2.0 nm) and one 2:1 silicate layer with an expanded $n_C = 18$ interlayer (1.4 nm), as a low-charge smectite would expand to at least 1.77 nm after treatment with $n_C = 18$ cations (Table 1). Lattice-fringe images of the 2:1 clay minerals of this sample, however, do not show R1 layer structures (see below). The reflection of 1.92 nm may represent a bilayer to pseudotrimolecular arrangement of alkyl chains in the interlayer space of a low-charge expandable 2:1 clay mineral. Hlavatý & Oya (1994) reported a $d(001)$ of 1.97 nm for a montmorillonite treated with $n_C = 18$.

The lattice-fringe images of the <0.05 μm fraction treated with $n_C = 8$ or $n_C = 18$ from 1463.0 m (and 1935.4 m: see below) depth generally show (Figs. 6a, b): (1) curved layers of short length that cluster in areas with a high degree of layer disorganization, in which low-charge 2:1 clay minerals appear as single units or sequences of layers with variable or irregular spacing, and are considered as smectite, (2) sequences of curved to planar, subparallel 2:1 silicate layers having expanded and variable interlayer spacing up to ~3.0 nm, considered as a high-charge 2:1 clay mineral (smectite or vermiculite), (3) isolated double layers (two 2:1 silicate layers with a contracted interlayer), and (4) apparently coherent sequences (packets) of 2:1 clay minerals generally having more than six to eight contracted interlayers and characteristic of detrital illite or mica.

XRD analysis and TEM imaging of 2:1 clay minerals after treatment with n-alkylammonium cations: 1935.4 m

XRD analysis of the Mg-saturated and EG-solvated <0.05 μm clay separates from 1935.4 m suggests an R0 illite(0.50)/EG-smectite. The diffraction pattern of the <0.05 μm fraction from 1935.4 m after treatment with $n_C = 8$ is similar to the pattern from 1463.0 m, except that the broad composite reflection ($001_{1.77}$/$001_{1.36}$/$001_{1.0}$) has shifted to a slightly higher 2θ angle, indicating a slight increase in the illite component (Fig. 5b). Comparison of the set of non-integral basal reflections of 1.36, 0.65, 0.46 and 0.334 nm with the XRD pattern of the air-dried sample shows a shift to lower-2θ angles, suggesting addition of a high-charge expandable 2:1 clay-mineral component, in addition to the low-charge smectite and illite layers. The diffraction pattern of the sample treated with $n_C = 18$ is similar to the samples above and below this depth. A sharp peak of 3.7 nm dominates, but in contrast to the sample from 1463.0 m, it has a better-resolved higher-order peak at 1.85 nm. The set of integral reflections of approximately 3.7 (001)*, 1.85 (002)* and 1.12 nm (003)* is consistent with either an R1 or R > 1 ordered structure. The R1 ordered structure would consist of one 2:1 silicate layer (= 1.0 nm) and one 2:1 silicate layer with an $n_C = 18$ expanded interlayer of 2.7 nm (1.0 + 2.7 = 3.7 nm). The intercalated $n_C = 18$ interlayer suggests an intermediate to high density of interlayer charge typical of vermiculite with a paraffin-type arrangement of the alkyl chains. An R > 1 ordered structure would consist of two 1.0 nm 2:1 silicate layers (2.0 nm) and one low-charge 2:1 silicate layer with a bilayer arrangement of $n_C = 18$ cations in the interlayer space (1.7 nm). Vali & Hesse (1992) had difficulty explaining the integral series of peaks of 3.6, 1.8 and 1.2 nm for Jefferson vermiculite treated with $n_C = 18$, and considered the possibility that polar molecules such as ethanol, used to remove excess alkylammonium salts and alkylamines after treatment, may aggregate to form clusters between the alkyl chains and result in anomalous expansion of the interlayer from the expected ~2.9 nm (Lagaly 1987). The 3.7 nm layer structure is, however, likely similar to the 3.4 nm layer

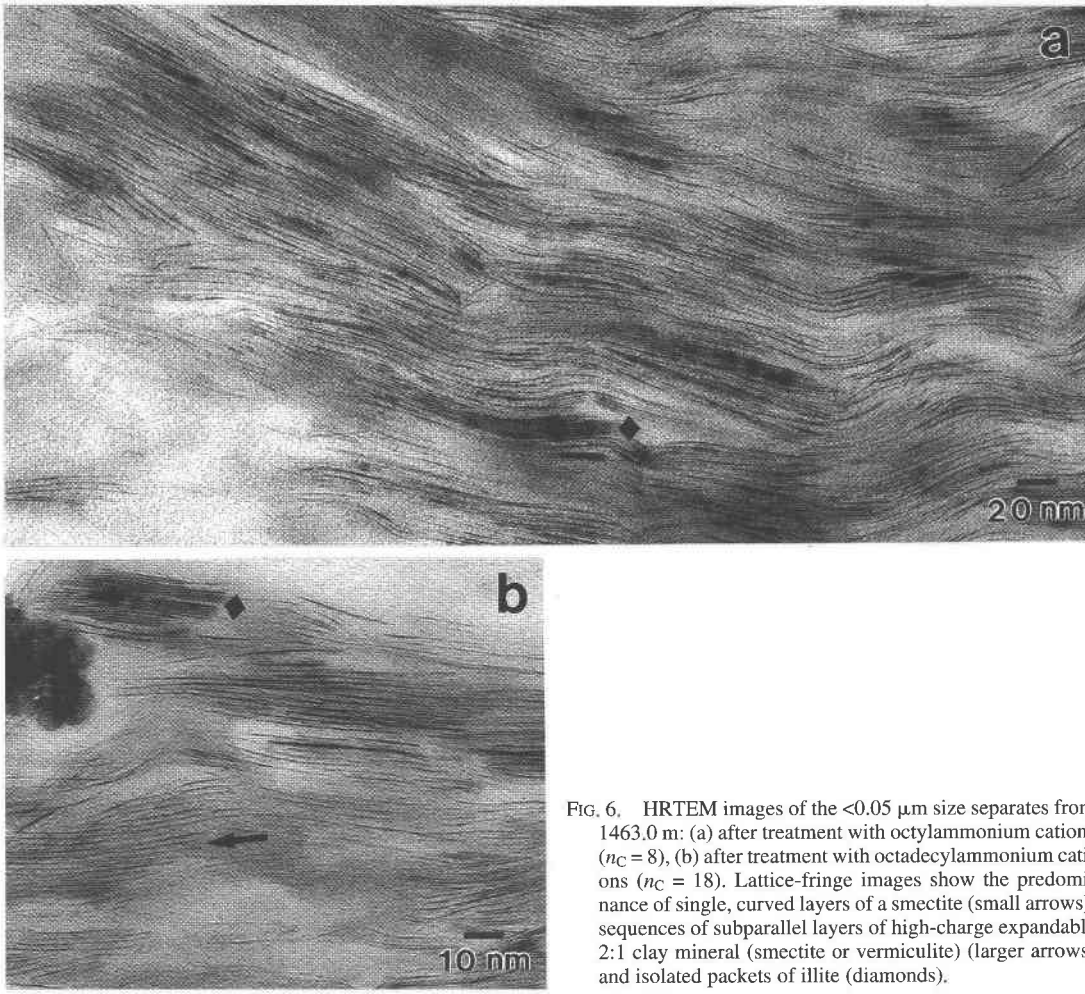

FIG. 6. HRTEM images of the <0.05 μm size separates from 1463.0 m: (a) after treatment with octylammonium cations (n_C = 8), (b) after treatment with octadecylammonium cations (n_C = 18). Lattice-fringe images show the predominance of single, curved layers of a smectite (small arrows), sequences of subparallel layers of high-charge expandable 2:1 clay mineral (smectite or vermiculite) (larger arrows) and isolated packets of illite (diamonds).

structure identified in the XRD pattern of the sample from 1463.0 and considered an R1 phase.

XRD analysis and TEM imaging of 2:1 clay minerals after treatment with n-alkylammonium cations: 2659.4 m

XRD analysis of the Mg-saturated and EG-solvated sample from 2659.4 m suggests an R1 illite(0.65)/EG-smectite. The XRD pattern of the sample treated with n_C = 8 is similar to the patterns from 1463.0 m and 1935.4 m, with the broad composite ($001_{1.77}/001_{1.36}/001_{1.0}$) reflection, characteristic of the shallow samples, migrating to a higher-2θ angle as the amount of illite increased, and giving a set of reflections at 1.24, 0.48 and 0.335 nm (Fig. 5c). The XRD pattern of the sample treated with n_C = 18 is dominated by a series of relatively sharp reflections between 2° and 12° 2θ (Fig. 5c). The pattern is interpreted as consisting of two superstructures with sets of approximately integral reflections. The first set is 3.7 (001)*, 1.86 (002)*, 1.23 (003)*, 0.96 (004)*, 0.77 (005)*, 0.63 (006)*, and 0.57 (007)* nm. The reflections at 1.73, 1.28, 1.03, 0.743 nm may represent higher-order reflections, if we consider a superlattice [5.2 nm] (001)* peak, *i.e.*, [~5.2 nm] (001)* [2.6] (002)*, 1.73 (003)*, 1.28 (004)*, 1.03 (005)*, [0.87] (006)*, and 0.74 (007)* nm reflections (values in square brackets are inferred, not observed). As described in the previous section, the 3.7 nm structure is consistent with an R1 ordered layer-structure, and is observed in lattice-fringe images (see below). The ~5.2 nm superstructure is consistent with an R3 ordered layer-structure, also present in the sample from 3832.8 m. An R3 ordered layer-structure consists of three 1.0 nm 2:1 silicate layers (= 3.0 nm) and one 2:1 silicate layer with an interlayer expanded with n_C = 18 of ~2.2 nm. The intercalated n_C = 18 interlayer suggests an intermediate

interlayer-charge density typical of a vermiculite with a pseudotrimolecular or paraffin-type arrangement of n_C = 18 cations. This is consistent with the findings of Cetin & Huff (1995a), that the expandable interfaces of illite-rich IS have vermiculite-like interlayer-charge density.

Lattice-fringe images of the sample treated with n_C = 18 show (Figs. 7a, b): (i) the predominance of apparently coherent sequences of double layers with alternating contracted and expanded (with n_C = 18) interlayers, and considered as a rectorite-like R1 ordered phase (Vali *et al.* 1994), (ii) subordinate amounts of single layers of an expandable low-charge smectite-group mineral, (iii) minor amounts of sequences of a high-charge expandable 2:1 clay mineral, and (iv) isolated discrete packets of illitic clays containing three to six non-expanded interlayers. Vali *et al.* (1994) identified a rectorite-like R1 ordered layer-structure in lattice-fringe images of soil samples, which consists of sequences of double layers with alternating contracted and expanded (with n_C = 18) interlayers. The expanded layers have spacings of 2.5 and 3.0 nm (their Fig. 3b). This is consistent with a mean value of ~2.7 nm for the intercalated n_C = 18 interlayers (rectorite-like R1 ordered) component determined from XRD, *i.e.,* a superlattice reflection of 3.7 nm.

XRD analysis and TEM imaging of 2:1 clay minerals after treatment with n-alkylammonium cations: 3832.8 m

XRD analysis of the <0.05 μm fraction from 3832.8 m after Mg-saturation and EG-solvation suggests an R > 1 illite(80%)/EG-smectite. The diffraction pattern after treatment with n_C = 8 is characterized by a set of non-integral reflections of 1.13, 0.48, 0.45, and 0.336 nm (Fig. 5d). The pattern is similar to those of shallower depths except that the suggested broad composite ($001_{1.77}/001_{1.36}/001_{1.0}$) reflection has migrated to a higher-2θ angle as the amount of illite increased with burial depth. The XRD pattern of the sample treated with n_C = 18 is similar to that of the sample from 2659.4 m, except that only the R3 ordered, illitic phase is present (Fig. 5d). An R3 ordered layer-structure is suggested by apparently integral reflections of 1.73 (003)*, 1.04 (005)*, 0.87 (006)* and 0.74 (007)* nm, if we assume a superstructure of ~5.2 nm (001)*. Cetin & Huff (1995a) observed that only IS with approximately less than 10% expandable layers and treated with long-chain alkylammonium cations (n_C = 12) produced two characteristic reflections in XRD; a 1.0 nm peak represents contracted illite, and a >2.4 nm peak represents intercalated alkylammonium cations with a paraffin-type arrangement in the interlayers, which suggests a discrete, highly charged 2:1 clay mineral or segregated layers.

Lattice-fringe images of the <0.05 μm fraction after treatment with n_C = 8 and n_C = 18 show three different types of 2:1 clay minerals (Figs. 8, 9a, b, c): (i) predominantly discrete, contiguous to disorganized packets of illite containing two to six contracted interlayers with a nearly constant spacing of 1.0 nm (R3 ordered), (ii) minor amounts of apparently coherent sequences of parallel layers (packets) of an illitic phase having interlayers intercalated with n_C = 18 interlayers and a relatively uniform spacing of ~2.4–2.5 nm, and (iii) scattered double layers and sequences of double layers of a rectorite-like R1 ordered phase.

Implications of n-alkylammonium cation treatment for the evolution of S → I during burial diagenesis

The XRD patterns of oriented samples of both air-dried and Mg-saturated and glycol-solvated <0.05 μm fractions generally display reflections of weak intensity

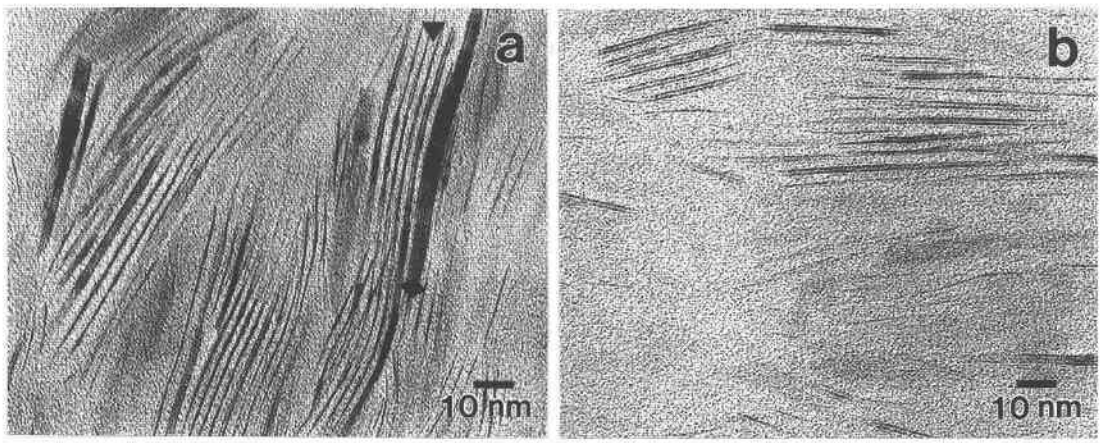

FIG. 7. HRTEM images of the <0.05 μm size fraction from 2659.4 m after treatment with n_C = 18: (a) packets of illite (diamonds), and (b) double layers and sequences of a short-range rectorite-like R1 ordered phase.

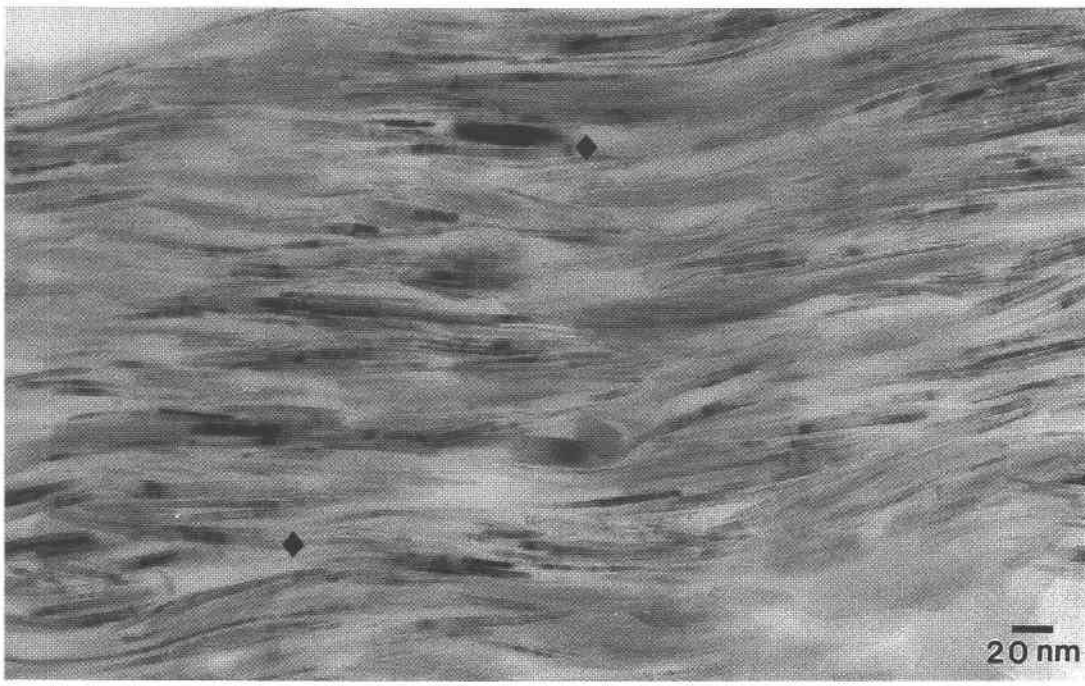

FIG. 8. HRTEM image of the <0.05 μm size fraction from 3832.8 m after treatment with $n_C = 8$ shows the predominance of packets of illite with two to six non-expanded interlayers (R3 ordered) (diamonds). Illite with interlayers intercalated with alkylammonium cations are not observed in samples treated with $n_C = 8$.

and unusual broadness in the present study. The experimental XRD patterns can be reasonably modeled by NEWMOD© using a simple two-component system of interstratified illite and smectite layers, with the percentage of illite layers increasing with depth of burial. Mg-saturation and glycerol solvation of the same size-fractions (Sears 1993), and the collapse of some expandable 2:1 layers after K^+-saturation to form illite-like layers in the <0.1 μm fractions (Ko & Hesse 1995), suggest that a third interstratified component, a high-charge expandable 2:1 clay-mineral component (smectite or vermiculite), is present in IS. But it is apparent that these treatments alone cannot reveal the true nature, structure and relationship of interstratified 2:1 clay minerals, the multiphase nature of illitic phases (rectorite-like R1 ordered, "*n*-alkylammonium illite", illite), nor the heterogeneity and complexity of 2:1 clay mineral assemblages that constitute the diagenetic evolution of S → I, especially in argillaceous sediments in the natural environment.

Some authors have questioned the conventional and often misleading notion that the evolution of S → I in diagenetic settings is a single, continuous and progressive reaction-series of intermediate IS interstratified structures with increasing temperature and burial depth. In an HRTEM study of ion-beam-milled IS samples from the Gulf of Mexico, Ahn & Peacor (1986a) demonstrated that the diagenetic evolution of S → I consisted of separate, discrete components of smectite and illite. Dong *et al.* (1997) were able to take this a step further by combining data from various geological settings to argue for the coexistence and simultaneous evolution of smectite, R1 IS, and illite with burial depth; owing to different methods of sample preparation, they could not directly compare their XRD and HRTEM results. However, because the technique of LR White resin cannot penetrate the interlayers of higher charge 2:1 clay minerals, these authors were unable investigate the multiphase nature of illite. By decomposing the polyphase IS XRD patterns of late-stage diagenetic assemblages from basins with low, constant geothermal gradients, Lanson *et al.* (1998) reported the simultaneous occurrence of three illitic phases, diagenetic IS, poorly crystallized illite, and a well-crystallized illite. In an XRD study of clay diagenesis in dacitic rock from Martinique under hydrothermal conditions, Bouchet *et al.* (1988a) reported the presence of multiphase IS assemblages (R0, R1 and R3 IS) that resulted from multiple reaction-series. In thermodynamic studies of smectite and IS, Aja & Rosenberg (1992) and Aja *et al.* (1991) proposed multiple, stoichiometric mica-like phases in the S → I reaction. As has been shown in the

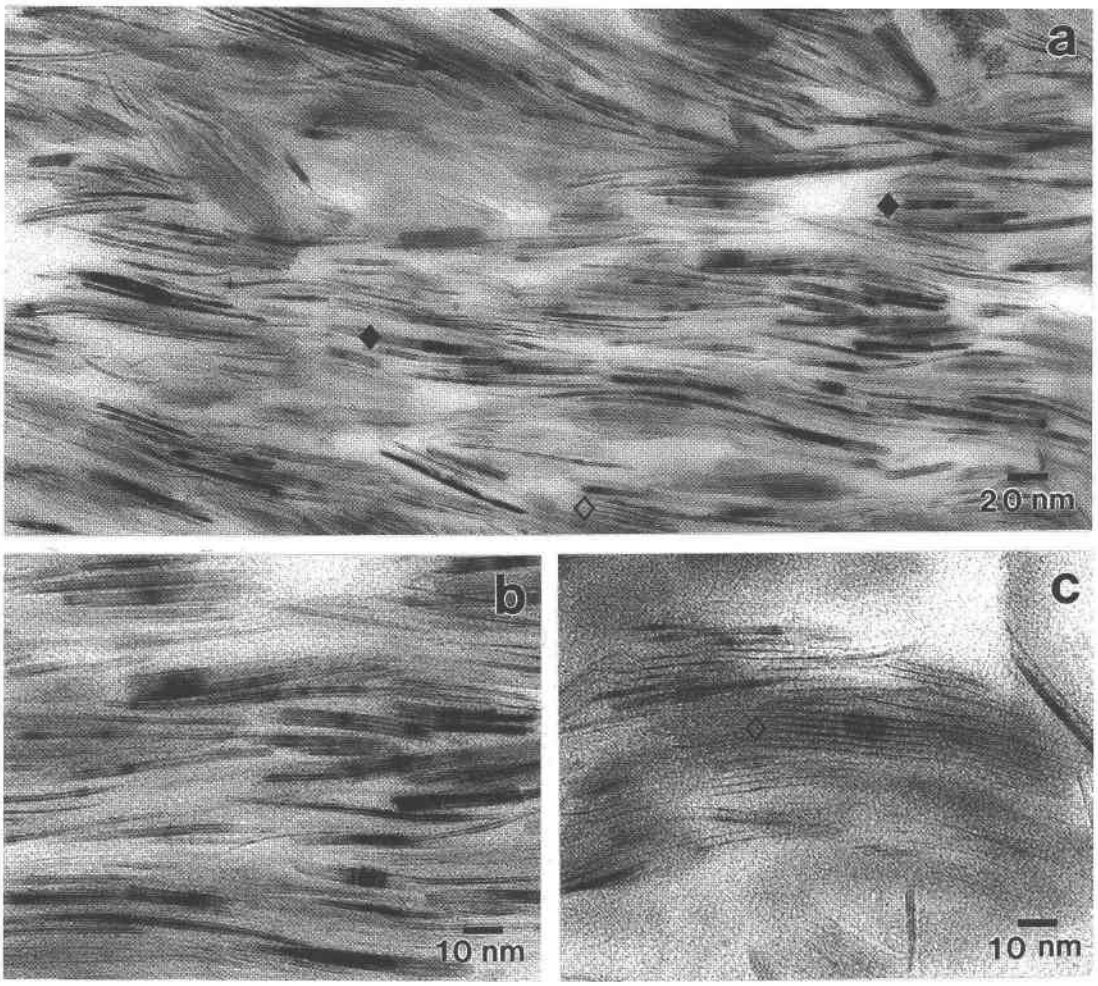

FIG. 9. HRTEM images of the <0.05 μm size fraction from 3832.8 m after treatment with n_C = 18: (a) overview showing the predominance of packets of illite with two to six contracted interlayers (R3 ordered), (b) close-up of (a) showing packets of illite (diamonds), and (c) packets of "octadecylammonium illite" with expanded interlayers (hollow diamonds).

present study in lattice-fringe images of 2:1 clay minerals after treatment with *n*-alkylammonium cations, these phases are actually the arrangement of different types of polar and nonpolar layers and not necessarily the various stacking sequences of illite and smectite layers (Vali *et al.* 1994).

The XRD patterns of the 2:1 clay minerals in the <0.05 μm fraction of the present study treated with *n*-alkylammonium cations generally show sharper peaks than their air-dried and EG-solvated counterparts (Figs. 5a, b, c, d). Although XRD analysis of the <0.05 μm fraction after treatment with n_C = 8 and n_C = 18 provides information on the layer sequences and mineralogical character of the 2:1 clay minerals with increasing temperature and depth of burial, *e.g.*, R1 and R3 ordered illitic phases in the intermediate and deep subsurface samples, the generally complex series of reflections in XRD patterns are difficult to interpret without lattice-fringe images obtained from TEM of the same size-fractions after treatment with *n*-alkylammonium cations.

Lattice-fringe images of the <0.05 μm fraction after treatment with *n*-alkylammonium cations directly reveal the heterogeneous and mutable multiphase nature of the 2:1 clay mineral assemblages that constitute the evolution of S → I in argillaceous rocks of the Reindeer D–27 well. In the prediagenetic and early stages (shallow depth), four distinct phases are present: (i) dispersed single layers of low-charge smectite are predominant, (ii) sequences of curved, subparallel expanded layers of

a high-charge expandable 2:1 clay mineral (smectite or vermiculite) are subordinate, (iii) double layers of a rectorite-like R1 ordered phase are dispersed, and (iv) packets of an illitic or micaceous phase with generally more than six to eight layers and considered detrital in origin are isolated. In the intermediate stage (i), the rectorite-like R1 ordered phase is predominant, (ii) with lesser amounts of sequences of a high-charge expandable 2:1 clay mineral, (iii) subordinate single layers of a low-charge smectite, and (iv) scattered packets of illite containing two to six contracted interlayers. The late stage is characterized by (i) the predominance of packets of illite with two to six contracted interlayers, (ii) subordinate amounts of packets of "octadecylammonium illite", and (iii) dispersed double layers of a rectorite-like R1 ordered phase.

Thus, the overall impression emerging from the present study of the diagenetic evolution of S → I in argillaceous rocks of the MDBS region is similar to that gained in other studies of clay-mineral diagenesis in passive continental margin settings. An initially heterogeneous mixture of clay minerals dominated by smectite-rich material at shallow depths evolves into multiphase illitic material with increasing time, temperature, and depth of burial. It is apparent that kinetic factors may be responsible for the persistence and coexistence of 2:1 clay mineral assemblages in zones that overlap with increasing time, temperature and depth of burial (Lippman 1982, May *et al.* 1986, Jiang *et al.* 1990, Whitney & Northrop 1988, Lanson & Champion 1991, Freed & Peacor 1992). Sears *et al.* (1998) presented lattice-fringe images that show illitic or micaceous components undergoing dissolution. It is likely, therefore, that the detrital component is metastable and dissolves with depth, providing K and Al for the formation of diagenetic illite. Thinner packets of illite, however, also exist at shallow depths; these may be diagenetic in origin. TEM images of Pt–C replicas show smectite particles occurring as anhedral flakes of a single-layer thickness, which correspond to the dispersed single-layers observed in the lattice-fringe images (Sears *et al.* 1998). Thicker crystallites of illite were observed as subhedral lath-like and anhedral particles, and likely correspond to the packets of illite observed in the lattice-fringe images. On the basis of morphology, it is likely that the subhedral laths of illite are authigenic, whereas the anhedral particles are detrital (Inoue *et al.* 1987, Lanson & Champion 1991). Freed & Peacor (1992) observed euhedral crystallites of illite in the <2.0 μm fraction of pre-transition smectite-rich material, and concluded that the small crystallites of illite are authigenic; they developed at low temperatures and shallow depths. Sears *et al.* (1998) presented K–Ar dating of the <0.05 μm clay mineral separates, which suggests that an authigenic component of illite is formed at relatively shallow depths, and that a component of detrital illite is always present during the evolution of S → I in argillaceous rocks of the Reindeer D–27 well.

Single layers of a low-charge smectite or expanded sequences of a high-charge expandable 2:1 clay mineral after treatment with $n_C = 8$ were not observed in the lattice-fringe images of samples at this depth, although the XRD pattern of the Mg-saturated, EG-solvated sample at this depth suggests a smectite component of about ~20%. Sears *et al.* (1998) presented TEM images of Pt–C replicas that show illite crystallites with subhedral lath-like and equidimensional or pseudohexagonal habit, which correspond to the packets of illite observed in the lattice-fringe images. The relatively uniform thickness of the packets of illite (Figs. 8a, b, c) and their subhedral and euhedral habit suggest that illite at maximum subsurface depth is largely diagenetic. Varajão & Meunier (1995) observed from TEM images that although the proportion of metastable laths decreases with depth in shales with respect to isometric (pseudohexagonal) particles, both continue to grow simultaneously at depth. Lanson & Champion (1991) concluded that illite developed as hexagonal particles is the stable phase in the diagenetic environment. Packets of "octadecylammonium illite", which were only recognized in lattice-fringe images of the present study in the sample from 3832.8 m, therefore must be a metastable phase. K–Ar dating of the <0.05 μm clay mineral separates suggests, however, that "octadecylammonium illite" exists in samples of all depths and is both detrital and diagenetic in origin (Sears *et al.* 1998).

More work is required in order to adequately quantify the abundance of each 2:1 clay mineral component at the various depths sampled using *n*-alkylammonium cation exchange. Although lattice-fringe images show that a high-charge expandable 2:1 clay mineral is subordinate to low-charge smectite at shallow depths, both phases are subordinate to the rectorite-like R1 ordered phase at intermediate depths, and neither is observed in samples at maximum depth of the well; it is not possible to conclusively state that low-charge smectite converts to a high-charge expandable 2:1 clay mineral. Dioctahedral smectites of heterogeneous composition will react differently to changing conditions of time, temperature, or depth of burial (Bouchet *et al.* 1988a, b, Meunier *et al.* 1992). Whereas many investigators have suggested that layers of low-charge smectite react to form layers of high-charge smectite with increasing temperature (Howard & Roy 1985, Bell 1986, Inoue *et al.* 1987, Rask *et al.* 1997), others have concluded that in deep diagenetic settings, layers of low-charge smectite may react to form layers of high-charge smectite with quartz and kaolinite, whereas in surface or subsurface conditions, layers of high-charge smectite may react with quartz and kaolinite to form layers of low-charge smectite (Bouchet *et al.* 1988b, Meunier *et al.* 1992). However, as both types of expandable 2:1 clay minerals gradually disappear with depth, both must be considered metastable. A problem in recognizing these reactions is the presence of diagenetic phases such as the rectorite-like R1 ordered phase and the illitic phase

(R3 ordered), having interfaces (outer layers) with a vermiculite-like layer charge.

Temperature of illite formation

The BMB and BYB in the area of the Reindeer D–27 well (main delta region) are currently experiencing uplift and erosion (Issler & Katsube 1994). McNeil *et al.* (1996) concluded from vitrinite-reflectance data that the Tertiary section at Reindeer D–27 is thermally immature, with a low thermal-maturity gradient. Measured vitrinite-reflectance values of organic matter show a progressive increase with depth of burial, which generally parallels the trends of increasing numbers of illite layers in IS seen by XRD and K–Ar ages of illitic material in the <0.05 μm fractions (Sears *et al.* 1998). The mean maximum vitrinite-reflectance (VR_O) values range from 0.29 to 0.67% at 3226 m, and are projected to VR_O = 0.80% (logarithmic scale) at the base of the well at 3861.2 m (McNeil *et al.* 1996). The latter values suggest maximum paleotemperatures of between ~95° and 120°C (Barker & Pawlewicz 1986). The Tertiary paleogeothermal gradient for the BMB may resemble present-day values (Majorowicz & Dietrich 1989). Replotting the vitrinite-reflectance data from the Reindeer D–27 well at a linear scale (Gunther 1976, unpubl. data, retabulated by D.R. Issler and provided by D.H. McNeil, pers. commun., 1998) on the generalized diagram showing depth – vitrinite reflectance – geothermal gradient (Suggate 1998), suggests that ~1400 m, and perhaps upward of 1800 m, of erosion and uplift may have occurred in the sedimentary succession above the base of the Late Paleocene to Early Eocene Aklak Sequence (depth to which vitrinite reflectance data are available), with a paleogeothermal gradient of 26°C km^{-1}, which is similar to the present-day geothermal gradient (27 ± 5°C km^{-1}) calculated for Reindeer D–27 (J.A. Majorowicz, pers. commun., 1997) (Fig. 10). Major periods of erosion in the MDBS region may have occurred during the Late Albian – Early Cenomanian, Mid-Maastrichtian, Late Eocene and Late Miocene (Dixon *et al.* 1992a, b). The amount of erosion estimated from this diagram is greater than that projected from the shale-compaction curves of Issler (1992) for the main delta area of the MDBS region (<1000 m). Using the geothermal gradient obtained from Figure 10, the critical threshold paleotemperature for the onset of illite formation would be in the range of 70° to 85°C, which is consistent with temperatures determined for the IS reaction in other sedimentary basins (*e.g.*, North Sea: Glasmann *et al.* 1989, Giles *et al.* 1992; Gulf of Mexico: Freed & Peacor 1992).

Summary and Conclusions

1. The combination of XRD analysis and HRTEM imaging of 2:1 clay minerals after treatment with *n*-alkylammonium cations (n_C = 8, 18) can provide direct, detailed and accurate information on the nature and structure of the 2:1 clay mineral assemblages that constitute the diagenetic evolution of S → I in argillaceous rocks, which cannot be obtained from conventional treatments for XRD, such as ethylene glycol and glycerol that are used to assess expandability.

2. The relationship among the various 2:1 layer silicates in the <0.05 μm size-fraction separated from argillaceous rocks that constitute the diagenetic evolution of S → I in argillaceous rocks of the Reindeer D–27 well, MDBS region, is complex because of the persistence and coexistence of various metastable 2:1 layer silicates at various depths, including low-charge smectite, high-charge 2:1 clay mineral (smectite or vermiculite), rectorite-like R1 ordered phase (which

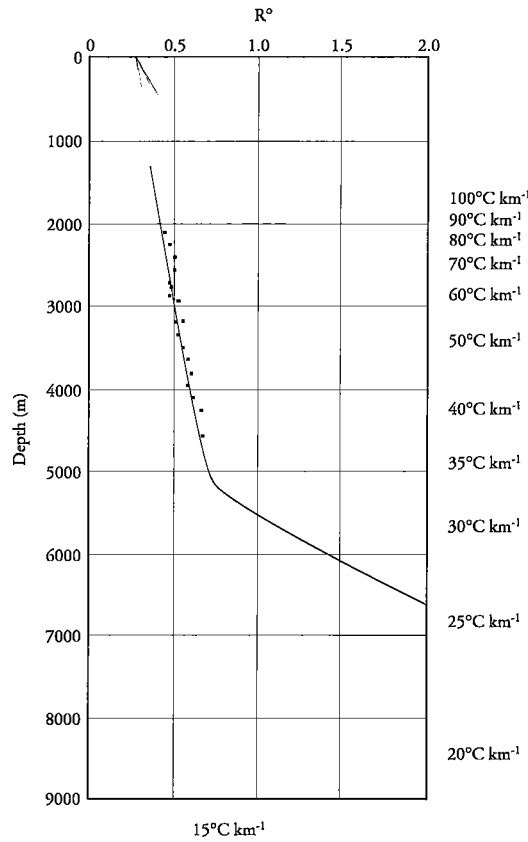

FIG. 10. The superposition of a linear plot of vitrinite reflectance values from the Reindeer D–27 well on a Depth – Vitrinite Reflectance – Geothermal Gradient diagram suggests that ~1400 m of erosion has occurred with a paleogeothermal gradient of ~ 26°C km^{-1}, which is comparable to the present-day geothermal gradient of 27 ± 5°C km^{-1} (J.A. Majorowicz, pers. commun., 1997). See Suggate (1998) for discussion of the method.

contains a high-charge expandable interlayer), "*n*-alkylammonium illite", and illite (with high-charge vermiculite-like interfaces), in addition to detrital micaceous phases, kaolinite (shallow), and chlorite (deep).

3. It is clear from the relationships of the 2:1 clay mineral assemblages in the lattice-fringe images and from TEM images of Pt–C replicas presented by Sears *et al.* (1998) that the diagenetic evolution of S → I cannot be considered as a single, continuous and progressive reaction-series, *i.e.*, a series of intermediate IS interstratified structures with increasing temperature and burial depth. Rather, the TEM images suggest the prograde sequence of discrete, multiphase assemblages that coexist in zones that overlap. In the early stages of S → I, simultaneous processes of dissolution and crystallization occur. Detrital illitic and micaceous particles and thin flakes of smectite-group minerals undergo dissolution, and particles of a rectorite-like R1 ordered phase and illite begin to precipitate. Although the rectorite-like R1 ordered phase dominates at intermediate depths, it is apparently not stable at greater depths, where laths and pseudohexagonal plates of illite predominate. In the Reindeer D–27 well, the illite began to precipitate in the temperature range between 70° and 85°C.

4. There is a probably a misperception in clay science that the application of *n*-alkylammonium cations to 2:1 clay minerals is a complicated and laborious procedure. This may be the case for the determination of the interlayer charge-density of expandable 2:1 clay minerals, which requires a series of treatments with alkylammonium cations of sequential chain-lengths. We advocate the use, however, of two or more of the commercially available alkylamine hydrochlorides (n_C = 8, 12, 18) to characterize the 2:1 clay minerals that comprise interstratified IS and the smectite-to-illite reaction in various geological settings.

Acknowledgements

This research was supported by grants from the Natural Sciences and Engineering Research Council (NSERC) of Canada (R.H. and H.V.) and the Petroleum Research Fund (PRF) administered by the American Chemical Society (ACS) (R.H.). S.K.S. thanks NSERC, Petro-Canada, Inc., and Fonds pour la Formation de Chercheurs et l'Aide à la Recherche (FCAR) Québec, for financially supporting his research through graduate scholarships. We are grateful to Gerhard Lagaly (Institut für anorganische Chemie der Universität Kiel), Paul H. Nadeau (Statoil), and Robert F. Martin (Department of Earth & Planetary Sciences, McGill University) for critically reading and suggesting improvements to an earlier version of this manuscript. We thank Mr. S. Tariq Ahmedali (Director, Geochemical Laboratories, McGill University) and Ms. Glenna Keating (Geochemical Laboratories, McGill University) for technical assistance.

References

Ahn, Jung-Ho & Peacor, D.R. (1986a): Transmission and analytical electron microscopy of the smectite-to-illite transition. *Clays Clay Minerals* **34**, 165-179.

_____ & _____ (1986b): Transmission electron microscope data for rectorite: implications for the origin and structure of "fundamental particles". *Clays Clay Minerals* **34**, 180-186.

Aja, S.U. & Rosenberg, P.E. (1992): The thermodynamic status of compositionally variable clay minerals: a discussion. *Clays Clay Minerals* **40**, 292-299.

_____, _____ & Kittrick, J.A. (1991): Illite equilibria in solutions. I. Phase relationships in the system K_2O–Al_2O_3–SiO_2–H_2O between 25°C and 250°C. *Geochim. Cosmochim. Acta* **37**, 542- 546.

Altaner, S.P. & Ylagen, R.F. (1997): Comparison of structural models of mixed-layer illite/smectite and reaction mechanisms of smectite illitization. *Clays Clay Minerals* **45**, 517-533.

Barker, C.E. & Pawlewicz, M.J. (1986): The correlation of vitrinite reflectance with maximum temperature in humic organic matter. *In* Lecture Notes in Earth Sciences. 5. Paleogeothermics: Evaluation of Geothermal Conditions in the Geological Past (G. Buntebarth & L. Stegena, eds.). Springer-Verlag, Berlin, Germany (79-93).

Bell, T.E. (1986): Microstructures in mixed-layer illite–smectite and its relationship to the reaction of smectite to illite. *Clays Clay Minerals* **34**, 146-154.

Bouchet, A., Meunier, A. & Velde, B. (1988a): Hydrothermal mineral assemblages containing two discrete illite/smectite minerals. *Bull. Minéral.* **111**, 587-599.

_____, Proust, D., Meunier, A. & Beaufort, D. (1988b): High-charge to low-charge smectite reaction in hydrothermal alteration processes. *Clay Mineral.* **23**, 133-146.

Cetin, K. & Huff, W.D. (1995a): Layer charge of the expandable component of illite/smectite in K-bentonite as determined by alkylammonium ion exchange. *Clays Clay Minerals* **43**, 150-158.

_____ & _____ (1995b): Characterization of untreated and alkylammonium ion exchanged illite/smectite by high resolution transmission electron microscopy. *Clays Clay Minerals* **43**, 337-345.

Chamney, T.P. (1971): Tertiary and Cretaceous biostratigraphic divisions in the Reindeer D–27 borehole, Mackenzie River Delta. *Geol. Surv. Can., Pap.* **70-30**.

Dietrich, J.R. & Dixon, J. (1997): Geology of the Beaufort Sea continental shelf. *In* Geology and Mineral and Hydrocarbon Potential of Northern Yukon Territory and Northwestern District of Mackenzie (D.K. Norris, ed.). *Geol. Surv. Can., Bull.* **422**.

_____, _____ & MCNEIL, D.H. (1985): Sequence analysis and nomenclature of Upper Cretaceous to Holocene strata in the Beaufort–Mackenzie Basin. *Geol. Surv. Can., Pap.* **85-1A**, 613- 628.

_____, _____, _____ & SNOWDON, L.R. (1989): Geology, biostratigraphy and organic geochemistry of strata in the Beaufort–Mackenzie area, Arctic Canada. *Can. Soc. Petroleum Geol., Short Course Supplementary Notes.*

DIXON, J. (1990): Stratigraphic tops in wells from the Beaufort–Mackenzie area, northwest Canada. *Geol. Surv. Can., Open File* **2310**.

_____, DIETRICH, J.R. & MCNEIL, D.H. (1992a): Upper Cretaceous to Pleistocene sequence stratigraphy of the Beaufort–Mackenzie and Banks Island areas, northwest Canada. *Geol. Surv. Can., Bull.* **407**.

_____, _____, _____, MCINTYRE, D.J., SNOWDON, L.R. & BROOKS, P. (1985): Geology, biostratigraphy and organic geochemistry of Jurassic to Pleistocene strata, Beaufort–Mackenzie area, northwest Canada. *Can. Soc. Petroleum Geol., Course Notes.*

_____, _____, SNOWDON, L.R., MORELL, G. & MCNEIL, D.H. (1992b): Geology and petroleum potential of Upper Cretaceous and Tertiary strata, Beaufort–Mackenzie area, northwest Canada. *Am. Assoc. Petroleum Geol., Bull.* **76**, 927-947.

_____, MORELL, G.R., DIETRICH, J.R., TAYLOR, G.C., PROCTER, R.M., CONN, R.F., DALLAIRE, S.M. & CHRISTIE, J.A. (1994): Petroleum resources of the Mackenzie Delta and Beaufort Sea. *Geol. Surv. Can., Bull.* **474**.

DONG, HAILIANG, PEACOR, D.R. & FREED, R.L. (1997): Phase relations among smectite, R1 illite–smectite, and illite. *Am. Mineral.* **82**, 379-391.

DREVER, J.I. (1973): The preparation of oriented clay mineral specimens for X-ray diffraction analysis by a filter-membrane peel technique. *Am. Mineral.* **58**, 553-554.

FREED, R.L. & PEACOR, D.R. (1992): Diagenesis and the formation of authigenic illite-rich I/S crystals in Gulf Coast shales: TEM study of clay separates. *J. Sed. Petrol.* **62**, 220-234.

GILES, M.R., STEVENSON, S., MARTIN, S.V., CANNON, S.J.C., HAMILTON, P.J., MARSHALL, J.D. & SAMWAYS, G.M. (1992): The reservoir properties and diagenesis of the Brent Group: a regional perspective. *In* Geology of the Brent Group (A.C. Morton, R.S. Haszeldine, M.R. Giles & S. Brown, eds.). *Geol. Soc., Spec. Publ.* **61**, 289-327.

GLASMANN, J.R., LARTER, S., BRIEDIS, N.A. & LUNDEGARD, P.D. (1989): Shale diagenesis in the Bergen High area, North Sea. *Clays Clay Minerals* **37**, 97-112.

GUNTHER, P.R. (1976): Palynomorph color and dispersed coal particle reflectance from three Mackenzie Delta boreholes. *Geoscience of Man* **15**, 35-39.

GUTHRIE, G.D., JR. & VEBLEN, D.R. (1989): High-resolution transmission electron microscopy of mixed-layer illite/smectite: computer simulations. *Clays Clay Minerals* **37**, 1-11.

_____ & _____ (1990): Interpreting one-dimensional high-resolution transmission electron micrographs of sheet silicates by computer simulation. *Am. Mineral.* **75**, 276-288.

HLAVATÝ, V. & OYA, A. (1994): Intercalation of methacrylamide into sodium, calcium and alkylammonium-exchanged montmorillonites. *Appl. Clay Sci.* **9**, 199-210.

HOWARD, J.J. & ROY, D.M. (1985): Development of layer charge and kinetics of experimental smectite alteration. *Clays Clay Minerals* **33**, 81-88.

HOWER, J., ESLINGER, E.V., HOWER, M.E. & PERRY, E.A. (1976): Mechanism of burial metamorphism of argillaceous sediments: mineralogical and chemical evidence. *Geol. Soc. Am., Bull.* **87**, 725-737.

INOUE, A., KOHYAMA, N., KITAGAWA, R. & WATANABE, T. (1987): Chemical and morphological evidence for conversion of smectite to illite. *Clays Clay Minerals* **35**, 111-120.

ISSLER, D.R. (1992): A new approach to shale compaction and stratigraphic restoration, Beaufort–Mackenzie Basin and Mackenzie corridor, northern Canada. *Am. Assoc. Petroleum Geol., Bull.* **76**, 1170-1189.

_____ & KATSUBE, T.J. (1994): Effective porosity of shale samples from the Beaufort–Mackenzie Basin, northern Canada. *Geol. Surv. Can., Current Res.* **1994-B**, 19-26.

JAKOBSEN, H.J., NIELSEN, N.C. & LINDGREEN, H. (1995): Sequences of charged sheets in rectorite. *Am. Mineral.* **80**, 247-252.

JELETZKY, J.A. (1971): Marine Cretaceous biotic provinces and paleogeography of western and Arctic Canada, illustrated by a detailed study of ammonites. *Geol. Surv. Can., Pap.* **70-22**.

JIANG, WEI-TEH, PEACOR, D.R., MERRIMAN, R.J. & ROBERTS, B. (1990): Transmission and analytical electron microscope study of mixed-layer illite/smectite formed as an apparent replacement product of diagenetic illite. *Clays Clay Minerals* **38**, 449-468.

KO, J. (1992): *Illite/Smectite Diagenesis in the Beaufort–Mackenzie Basin, Arctic Canada.* Ph.D. thesis, McGill Univ., Montreal, Quebec.

_____ & HESSE, R. (1995): Mineralogy of illite/smectite mixed-layer clays from the Beaufort–Mackenzie Basin, Arctic Canada. *Econ. Environ. Geol.* **28**, 327-335.

_____ & _____ (1998): Illite/smectite diagenesis in the Beaufort–Mackenzie Basin, Arctic Canada: relation to hydrocarbon occurrence? *Bull. Can. Petroleum Geol.* **46**, 74-88.

LAGALY, G. (1979): The "layer charge" of regular interstratified 2:1 clay minerals. *Clays Clay Minerals* **27**, 1-10.

_____ (1981): Characterization of clays by organic compounds. *Clay Mineral.* **16**, 1-21.

_____ (1982): Layer charge heterogeneity in vermiculites. *Clays Clay Minerals* **30**, 215-222.

_____ (1987): Clay–organic interactions: problems and recent results. *Proc. Int. Clay Conf. (Tokyo)* **1**, 61-80.

_____ (1994): Layer charge determination by alkylammonium ions. *In* Layer Charge Characteristics of 2:1 Silicate Clay Minerals (A.R. Mermut, ed.). *Clay Mineral Soc., Workshop Lectures* **6**, 1-14.

_____ & WEISS, A. (1969): Determination of the layer charge in mica-type layer silicates. *In* Proc. Int. Clay Conf. 1 (Tokyo) (L. Heller, ed.). Israel Univ. Press, Jerusalem, Israel (61-80).

_____ & _____ (1970): Inhomogeneous charge distribution in mica-type layer silicates. *In* Reunión Hispano-Belga de Minerales de la Arcilla (Madrid) (J.M. Serratosa, ed.). *Consejo Cuperior de Investigaciones Cientificas, Madrid, Spain* (179-187).

LAIRD, D.A. (1994): Evaluation of structural formulae and alkylammonium methods of determining layer charge. *In* Layer Charge Characteristics of 2:1 Silicate Clay Minerals (A.R. Mermut, ed.). *Clay Mineral Soc., Workshop Lectures* **6**, 79-104.

_____ & NATER, E.A. (1993): Nature of illitic phase associated with randomly interstratified smectite/illite in soils. *Clays Clay Minerals* **41**, 280-287.

_____, SCOTT, A.D. & FENTON, T.E. (1987): Interpretation of alkylammonium characterization of soil clays. *Soil Sci. Soc. Am. J.* **51**, 1659-1663.

_____, THOMPSON, M.L. & SCOTT, A.D. (1989): Technique for transmission electron microscopy and X-ray powder diffraction analyses of the same clay mineral specimen. *Clays Clay Minerals* **37**, 280-282.

LANE, L.S. & DIETRICH, J.R. (1995): Tertiary structural evolution of the Beaufort Sea – Mackenzie Delta region, Arctic Canada. *Bull. Can. Petroleum Geol.* **43**, 293-314.

LANSON, B. & CHAMPION, D. (1991): The I/S-to-illite reaction in the late stage diagenesis. *Am. J. Sci.* **291**, 473-506.

_____, VELDE, B. & MEUNIER, A. (1998): Late-stage diagenesis of illitic clay minerals as seen by decomposition of X-ray diffraction patterns: contrasted behaviors of sedimentary basins with different burial histories. *Clays Clay Minerals* **46**, 69-78.

LEE, S.Y., JACKSON, M.L. & BROWN, J.L. (1975): Micaceous occlusions in kaolinite observed by ultramicrotomy and high-resolution electron microscopy. *Clays Clay Minerals* **23**, 125-129.

LIPPMAN, F. (1982): The thermodynamic status of clay minerals. *In* Proc. 8th Inter. Clay Conf, 1981 (H. van Olphen & F. Veniale, eds.). Elsevier, New York, N.Y. (475-485).

_____ & JOHNS, W.D. (1969): Regular interstratification in rhombohedral carbonates and layer silicates. *Neues Jahrb. Mineral. Geol. Paläont., Monatsh.*, 212-221.

MACKINTOSH, E.E. & LEWIS, D.G. (1968): Displacement of potassium from micas by dodecylammonium chloride. *Trans. 9th Int. Congress Soil Sci. (Adelaide)* **2**, 696-703.

_____, _____ & GREENLAND, D.J. (1971): Dodecylammonium–mica complexes. I. Factors affecting the exchange reaction. *Clays Clay Minerals* **19**, 209-218.

_____, _____ & _____ (1972): Dodecylammonium–mica complexes. II. Characterization of the reaction products. *Clays Clay Minerals* **20**, 125-134.

MAJOROWICZ, J.A. & DIETRICH, J.R. (1989): Comparison of the geothermal and organic maturation gradients of the central and southwestern Beaufort–Mackenzie Basin, Yukon and Northwest Territories. *Geol. Surv. Can., Pap.* **89-1**, 63-67.

MALLA, P.B. & DOUGLAS, L.A. (1987): Identification of expanding layer silicates: layer charge vs. expansion properties. *In* Proc. Int. Clay Conf. (Denver) (L.G. Schultz, H. van Olphen & F.A. Mumpton, eds.). The Clay Minerals Soc., Bloomington, Indiana (277-283).

_____, ROBERT, M., DOUGLAS, L.A., TESSIER, D. & KOMANRENI, S. (1993): Charge heterogeneity and nanostructure of 2:1 layer silicates by high-resolution transmission electron microscopy. *Clays Clay Minerals* **41**, 412-422.

MARCKS, C., WACHSMUTH, H. & REICHENBACH, H., GRAF VON (1989): Preparation of vermiculite for HRTEM. *Clay Mineral.* **24**, 23-32.

MAY, H.M., KINNIBURGH, D.G., HELMKE, P.A. & JACKSON, M.L. (1986): Aqueous dissolution, solubilities and thermodynamic stabilities of common aluminosilicate clay minerals: kaolinite and smectites. *Geochim. Cosmochim. Acta* **50**, 1667-1677.

MCALISTER, J.J. & SMITH, B.J. (1995): A rapid technique for X-ray diffraction analysis of clay minerals in weathered rock materials. *Microchem. J.* **52**, 53-61.

MCNEIL, D.H. (1997): New Foraminifera from the Upper Cretaceous and Cenozoic of the Beaufort–Mackenzie Basin of Arctic Canada. *Cushman Foundation for Foraminifera Research, Spec. Publ.* **35**.

_____, ISSLER, D.R. & SNOWDON, L.R. (1996): Colour alteration, thermal maturity and burial diagenesis in fossil foraminifers. *Geol. Surv. Can., Bull.* **499**.

MEUNIER, A., PROUST, D., BEAUFORT, D., LAJUDIE, A. & J.-C. PETIT (1992): Heterogeneous reactions of dioctahedral smectites in illite–smectite and kaolinite–smectite mixed-layers: applications to clay materials for engineered barriers. *Appl. Geochem., Suppl. Issue* **1**, 143-150.

MOORE, D.M. & REYNOLDS, R.C., JR. (1997): *X-Ray Diffraction and Identification and Analysis of Clay Minerals* (2nd ed.). Oxford University Press, New York, N.Y.

MÜLLER-VONMOOS, M., KAHR, G. & MADSEN, F.T. (1994): Intracrystalline swelling of mixed-layer illite–smectite in K-bentonites. *Clay Mineral.* **29**, 205-213.

NADEAU, P.H., WILSON, M.J., MCHARDY, W.J. & TAIT, J.M. (1985): The conversion of smectite to illite during diagenesis: evidence from some illitic clays from bentonites and sandstones. *Mineral. Mag.* **49**, 393-400.

POLLASTRO, R. (1982): A recommended procedure for the preparation of clay mineral specimens for X-ray diffraction analysis – modification to Drever's filter membrane peel technique. *U.S. Geol. Surv., Open File Rep.* **82-71**.

_____ (1985): Mineralogical and morphological evidence for the formation of illite at the expense of illite/smectite. *Clays Clay Minerals* **33**, 265-274.

POWELL, T.G., FOSCOLOS, A.E., GUNTHER, P.R. & SNOWDON, L.R. (1978): Diagenesis of organic matter and fine clay minerals: a comparative study. *Geochim. Cosmochim. Acta* **42**, 1181-1197.

RASK, J.H., BRYNDZIA, L.T., BRAUNSDORF, N.R. & MURRAY, T.E. (1997): Smectite illitization in Pliocene-age Gulf of Mexico mudrocks. *Clays Clay Minerals* **45**, 99-109.

REYNOLDS, R.C., JR. (1985): *NEWMOD©, a Computer Program for the Calculation of One Dimensional Diffraction Patterns of Mixed-Layered Clays.* R.C. Reynolds, Jr., 8 Brook Road, Hanover, New Hampshire 03755, U.S.A.

ROSS, G.J. & RICH, C.I. (1973): Effect of particle thickness on potassium exchange from phlogopite. *Clays Clay Minerals* **21**, 77-81.

RÜHLICKE, G. & KOHLER, E.E. (1981): A simplified procedure for determining layer charge by the *n*-alkylammonium method. *Clay Mineral.* **16**, 305-307.

SEARS, S.K. (1993): *Effects of Sample Treatment on Mixed Layer Illite–Smectite Revealed by X-Ray Diffractograms and Transmission Electron Micrographs.* M.Sc. thesis, McGill Univ., Montreal, Quebec.

_____, HESSE, R., VALI, H., ELLIOTT, W.C. & ARONSON, J.L. (1995a): K–Ar dating of illite diagenesis in ultrafine fractions of mudrocks from the Reindeer D–27 well, Beaufort–Mackenzie area, Arctic Canada. *In* Proc. 8th Int. Symp. on Water–Rock Interaction (Vladivostok) (Y.K. Kharaka & O.V. Chudaev, eds.). Balkema, Rotterdam, The Netherlands (105-108).

_____, _____, _____, _____ & _____ (1995b): A new approach to differentiate between detrital and diagenetic illitic material. *In* Euroclay '95, Clays and Clay Materials Sciences (Leuven) (A. Elsen, P. Grobet, M. Keung, H. Leeman, R. Schoonheydt & H. Toufar, eds.). (381-383).

_____, _____, _____, _____, _____ & MARTIN, R.F. (1998): K–Ar ages of 2:1 clay minerals, Mackenzie Delta – Beaufort Sea region, Arctic Canada: significance of *n*-alkylammonium exchange. *Can. Mineral.* **36**, 1507-1524.

SPURR, A.R. (1969): A low viscosity epoxy resin embedding medium for electron microscopy. *J. Ultrastr. Res.* **26**, 31-43.

STANJEK, H., NIEDERBUDDE, E.A. & HÄUSLER, W. (1992): Improved evaluation of layer charge of *n*-alkylammonium-treated fine soil clays by Lorentz- and polarization-correction and curve-fitting. *Clay Mineral.* **27**, 3-19.

ŠUCHA, V., KRAUS, I., GERTHOFFEROVÁ, H., PETEŠ, J. & SEREKOVÁ, M. (1993): Smectite to illite conversion in bentonites and shales of the East Slovak Basin. *Clay Minerals* **28**, 243-253.

SUDO, T., HAYASI, H. & SHIMODA, S. (1962): Mineralogical problems of intermediate clay minerals. *Clays Clay Mineral.* **9**, 378-392.

SUGGATE, R.P. (1998): Relations between depth of burial, vitrinite reflectance and geothermal gradient. *J. Petroleum Geol.* **21**, 5-32.

TETTENHORST, R. & JOHNS, W.D. (1965): Interstratification in montmorillonite. *Clays Clay Minerals, Proc. 13th Natl. Conf. (Madison)*, 85-93.

VAIA, R.A., TEUKOLSKY, R.K. & GIANNELIS, E.P. (1994): Interlayer structure and molecular environment of alkylammonium layered silicates. *Chem. Mater.* **6**, 1017-1022.

VALI, H. & HESSE, R. (1990): Alkylammonium ion treatment ion treatment of clay minerals in ultrathin section: a new method for HRTEM examination of expandable layers. *Am. Mineral.* **75**, 1445-1448.

_____ & _____ (1992): Identification of vermiculite by transmission electron microscopy and X-ray diffraction. *Clay Mineral.* **27**, 185-192.

_____, _____ & KODAMA, H. (1992): Arrangement of alkylammonium ions in phlogopite and vermiculite: an XRD- and TEM-study. *Clays Clay Minerals* **40**, 240-245.

_____, _____ & KOHLER, E.E. (1991): Combined freeze-etched replicas and HRTEM images as tools to study fundamental-particles and multi-phase nature of 2:1 layer silicates. *Am. Mineral.* **76**, 1953-1964.

_____, _____ & MARTIN, R.F. (1994): A TEM-based definition of 2:1 layer silicates and their interstratified constituents. *Am. Mineral.* **79**, 644-653.

_____ & KÖSTER, H.M. (1986): Expanding behavior, structural disorder, regular and random irregular interstratification of 2:1 layer silicates studied by high-resolution images of transmission electron microscopy. *Clay Mineral.* **21**, 827-859.

VARAJÃO, A. & MEUNIER, A. (1995): Particle morphological evolution during the conversion of I/S to illite in lower Creatceous shales from Sergipe–Alagoas Basin, Brazil. *Clays Clay Minerals* **43**, 14- 28.

VEBLEN, D.R., GUTHRIE, G.D., JR., LIVI, K.J.T. & REYNOLDS, R.C., JR. (1990): High-resolution transmission electron microscopy and electron diffraction of mixed-layer illite/smectite: experimental results. *Clays Clay Minerals* **38**, 1-13.

VELDE, B. (1985): *Clay Minerals. A Physico-Chemical Explanation of their Occurrence*. Elsevier Developments in Sedimentology **40**, New York, N.Y.

VON REICHENBACH, H. GRAF (1973): Exchange equilibria of interlayer cations in different particle size fractions of biotite and phlogopite. *In* Proc. Int. Clay Conf. (Madrid) (J.M. Serratosa & A. Sánchez, eds.). Division de Ciencias C.S.I.C., Madrid, Spain (457-466).

WEISS, A. (1963): Mica-type layer silicates with alkylammonium ions. *Clays Clay Minerals* **10**, 191- 224.

_____, HOLM, C. & PLATIKANOV, D. (1993): Phase studies of long-chain alkanol complexes with alkylammonium layer silicates. *Colloid Polymer Sci.* **271**, 891-900.

WHITNEY, G. & NORTHROP, H.R. (1988): Experimental investigation of the smectite to illite reaction: dual reaction mechanisms and oxygen-isotope systematics. *Am. Mineral.* **73**, 77-90.

YOUNG, F.G., MYHR, D.W. & YORATH, C.J. (1976): Geology of the Beaufort–Mackenzie Basin. *Geol. Surv. Can., Pap.* **76-11**.

Received February 19, 1998, revised manuscript accepted October 5, 1998.